DOI:10.14753/SE.2022.2689

Biomechanical and clinical aspects in special forms of intervertebral disc degeneration

PhD thesis

László Kiss, MD

Károly Rácz Doctoral School of Clinical Medicine

Semmelweis University

Supervisor: Áron Lazáry, MD, Ph.D

Official reviewers: Szabolcs Molnár, MD, Ph.D
Gergely Holnapy, MD, Ph.D

Head of the Final Examination Committee:
György Szőke MD, D.Sc

Members of the Final Examination Committee:
György Márk Hangody, MD, Ph.D
Tamás Terebessy, MD, Ph.D

Budapest
2022

DOI:10.14753/SE.2022.2689

Table of contents

DOI:10.14753/SE.2022.2689

List of Abbreviations

AF	annulus fibrosus
ASD	adjacent segment degeneration
ASDeg	radiologic adjacent segment degeneration
ASDis	symptomatic adjacent segment degeneration
C	cervical
CT	computer tomography
DHA	disc height anterior
DHP	disc height posterior
ECM	extracellular matrix
FEM	finite element modelling
GAG	glycosaminoglycans
IPH	interpedicular height
IVD	intervertebral disc
L	lumbar
LBP	low back pain
LL	lumbar lordosis
LP	leg pain
LS	lumbar scoliosis
MIS	minimally invasive surgery
MRI	magnetic resonance imaging
NP	nucleus pulposus
ODI	Oswestry Disability Index
PI-LL	pelvic incidence - lumbar lordosis mismatch
PCD	percutaneous cement discoplasty
PG	proteoglycans
PI	pelvic incidence
PMMA	polymethyl methacrylate
PROM	patient related adjacent segment degeneration
PT	pelvic tilt
RCT	randomised controlled trial
SS	sacral slope

sS	segmental scoliosis
T1-WI	T1 weighted imaging
T2-WI	T2 weighted imaging
Th	thoracic
VAS	visual analogue scale
TLIF	transforaminal lumbar interbody fusion
sLoF	segmental lordosis of fusion
sL	segmental lordosis
HD	Hausdorff distance
ICC	intraclass correlation coefficient
ANOVA	analysis of variance
M	male
F	female
6M FU	6 months’ follow-up
FU	follow-up
BMI	body mass index
OR	odds ratio
ROM	range of motion

DOI:10.14753/SE.2022.2689

1. Introduction and background

Low back pain (LBP) is a common health problem and major cause of disability. LBP is responsible for the highest disability-adjusted life-years globally, it affects people from children to elderly [1]. Worldwide, 266 million individuals (3.63%) suffer from degenerative spinal disease and related LBP yearly [2]. The better understanding of the role of intervertebral disc as a main spinal element may improve spinal care.

This dissertation focuses on two specific disc degeneration related conditions that have a great impact on clinical management and long-term surgical outcome.

Our first aim was, to study advanced stage disc degeneration with total disc collapse, vacuum phenomenon, multiplex osteophytes and severe neuroforaminal stenosis. These conditions contribute to poor quality of life and severe disabilities and may require spinal surgeries.

Second aim was to investigate factors, that may affect the adjacent levels and discs leading to adjacent segment degeneration (ASD) after instrumented spinal stabilisation surgeries. ASD related pain and disabilities are one of the main reasons of revision surgeries worldwide. Factors leading to ASD have been studied extensively, but the aetiology still remains unclear.

DOI:10.14753/SE.2022.2689

1.1. The intervertebral disc

1.1.1. Embryology and anatomy

The symphysis between the adjacent vertebral bodies is the intervertebral disc (IVD). This anatomical and functional unit is formed by the surrounding fibrocartilaginous adjacent vertebral endplates, central highly hydrated nucleus pulposus, and concentric-layered surrounding structure, the annulus fibrosus. (**Figure 1**)

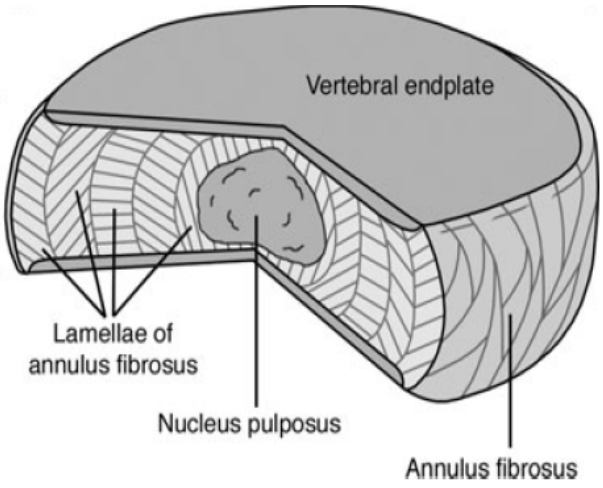

Figure 1. Structure of IVD

The figure shows the main anatomical structures of an intervertebral disc [3].

The formation of IVD from embryonic layers occurs in the third gestational week. During gastrulation, future ectoderm cells colonize the mesoblastic space to form the notochord (axial mesoderm). The development of the notochord is depending on the expression of specific genes (Foxa2, Brachyury, Noto). Adjacent to notochord, pararaxial mesoderm forms somites, which contains sclerotome cells. These cells condense around the notochord and give rise to the vertebrae, endplates, and annulus fibrosus (AF) of the intervertebral disc, while the nucleus pulposus of the disc arises from the notochord [4–6]. (**Figure 2**)

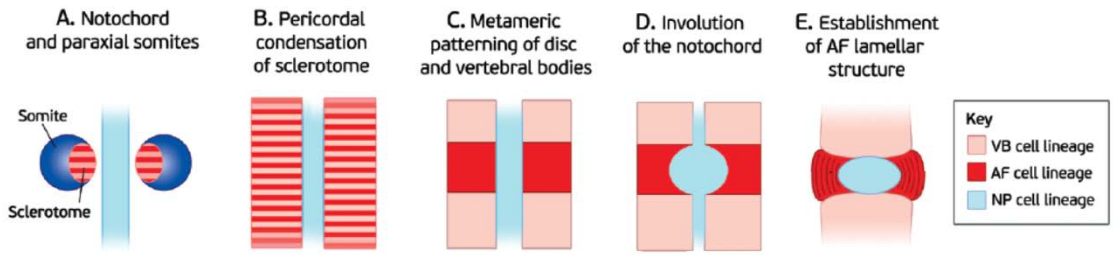

Figure 2. Embryonic morphogenesis of the intervertebral disc

A *Notochord and adjacent somites* ***B*** *Sclerotome cells condense around the notochord* ***C*** *Cells adopt a metameric pattern of more condensed regions give a rise to vertebral bodies* ***D*** *Notochord contacts with vertebral body and expands to nucleus pulposus* ***E*** *Basic structure of the IVD. Figure adapted from Tomaszewski et al. [5].*

Vertebral endplates are built up by two main layers, the subchondral bone and a thin, approximately 1 mm thick hyaline cartilage. This cartilage contains chondrocytes synthetizing extracellular matrix (ECM), mostly collagen II, proteoglycans (PGs) and glycosaminoglycans (GAG). These fibers run horizontal and parallel to the vertebral bodies anchoring the AF to the endplate. The nutritional intake during the development and growth of the disc takes place in microscopic network of blood vessels, where metabolites diffuse through pores based on their size and charge. Only positive ions (e.g., sodium, calcium) or neutral molecules, such as glucose and oxygen can diffuse [3,6].

Annulus fibrosus consists of fibroblasts and ECM structured into lamellae with 15-25 concentric layers. These lamellae are interconnected by PGs aggregate and lubricin to reduce the friction between adjacent lamellaes. There are two main parts of the annulus, the inner and the outer. The inner part has less organised ECM, with mainly type II collagen, PGs and high water content. The outer part consists of mostly type I collagen. From the inner to the outer part, the orientation of the collagen and elastin fibers change from 60-65˚ to vertical. This fibrosus structure yields important

mechanical properties as the outer AF has a higher tension resistance, which limits nucleus pulposus protrusion [3,6,7].

The central area of the intervertebral disc is the nucleus pulposus (NP) surrounded by annular fibers. NP is composed of several cell types (notochordal cells, chondrocyte-like cells, mesenchymal stem cells) that are embedded in a matrix. The ECM consists of type II collagen and aggrecan with sulphated GAGs. The negative charges of GAGs maintain high osmotic pressure and are responsible for the high water content that contributes to the absorption of spinal loads [8]. Due to the specific circumstances of the nutrition of intervertebral disc, NP cells are highly specialised to survive in a hypoxic environment (1% of O_2). Notochondral cells play a key role in the NP. First, these cells produce growth-factors that stimulate the chondrocyte-like cells to synthetize the ECM (PGs, GAGs, collagen). In addition, these cells have the ability to prevent chondrocyte-like cells from apoptosis, by inhibiting the activation of apoptotic caspase cascade [3,6,7]. Taken together, it is emphasizes the fundamental role of notochordal cells in the survival and activity of chondrocyte-like cells, which subsequently maintain NP homeostasis [6].

1.1.2. Biomechanics

To maintain human posture, high loads are developed by the upper body and muscles of the back and exerted to the spine. These forces and loads increase as approaching the sacrum. The elements of the IVD are subjected to mechanical stimuli, such as tensile, compression, shear stresses and strains [9]. This complex structure was formed to adapt to mechanical functions, such as forces generated in flexion-extension, bending, rotations and compressive loads. Spinal motion segment as a biomechanical unit grants 6 degrees of freedom in flexion-extension, lateral bending and rotation. These complex movements require both the morphological structure and the biochemical composition of the disc’s matrix and lamellar structure of the annulus [9]. In upright position, the axial load compresses the endplates resulting in deformation of the nucleus pulposus and along with the tension of the bulging AF. This deformation increases the internal hydrostatic pressure of the nucleus.[10] The increased pressure exerts the force was transmitted through the annulus fibrosus.

The variation of day and night activities produce a diurnal change in NP. As a result of upright position and repetitive loads, the intradiscal fluid is squeezed out of the disc

through the adjacent endplates into the vertebral bodies. The loss of fluid increases the PGs concentration as well as the osmolality and pH. In supine position, when the load decreases, negative pressure, and high osmolality brew the fluid back to the discs [8].
Posture dependent in vivo changes in intradiscal pressure was measured by Wilke et al. In their study, a pressure transducer was implanted to a healthy L4-5 disc of a volunteer. Intradiscal pressure slightly increased in extension compared to the neutral standing position, however the pressure increased exponentially with the increase of the angle in flexion. Lateral bending increased the pressure linearly, but over 20˚ it decreased both sides. One possible reason behind this phenomenon could be the active muscular stabilisation. Above 20˚ angle, the muscles release and the spine stabilises passively. Lifting a 20 kg object with both hands in front, knees bent and in upright posture with actively extended back multiplied the pressure by three times compered to neutral standing position. In contrast lifting with bent round back increased the pressure almost five times. Summarizing the study of Wilke et al., intradiscal pressure depends on the posture, the external load, muscle activity, the type of activity, and how it is carried out [11].

1.2. Degeneration process of the intervertebral disc

Biological ageing is an ongoing process; it could be described as the impact of molecular and cellular damage over time. As these harms accumulate, structural and functional changes may appear and develop over time. As a result of limited blood supply and nutrition, the intervertebral disc undergoes degeneration related changes earlier than other types of tissue.[12]

1.2.1. Nucleus pulposus and annulus fibrosus

In most of the cases, degeneration starts at the level of nucleus pulposus. As the cell content starts to reduce, change in the homeostasis of ECM is induced. In addition, an excessive catabolic activity can be observed in the regulation of catabolic and anabolic functions [13]. The decrease in matrix turnover and proteoglycan content lead to the loss of osmotic gradient, which is linked to reduction of swelling pressure [14]. This abnormal load distribution created by this process passes the pressure/force on to the annulus, which impacts the structure and morphology. As degeneration proceeds, the annulus fibrosus starts to act like a fibrosus solid and resists to compression directly

[15]. Increased stress can lead to further structural changes such as formation of fissures (circumferential, peripheral and radial) and annular tears [16]. Consequently, annular weakness and defects will develop and later segmental and spinal instability will occur. Circumferential fissures are the result of interlaminar shear stress, whereas peripheral defects are related to the bony outgrowth in the anterior part. Radial fissures are the most common in the posterior and posterolateral region of the disc. This type of defect is associated with degeneration and related to disc displacements such as herniation and protrusion [17,18]. All of the above mentioned changes are irreversible because the regeneration capacity of the disc is limited [17].

The above detailed alterations have clear signs on CT and MR images. The proteoglycan content within the nucleus correlates with the high signal intensity in T2-weighted sequence on MRI [19,20]. The loss of signal intensity correlates strongly with the progressive degeneration process. Pfirrmann et al. classified the disc degeneration into a five-grade scale based on the signal intensity of the NP and its' distinction of the AF [19]. As the degeneration tends to progress, the annular fibers show severe disorganisation, the nucleus dissolves and nitrogen accumulates within the disc. This vacuum phenomenon could be identified as a void gap in MRI either in T1 and T2-weighted images [21]. In CT scans these gas bubbles are visible as hypodense gaps. Vacuum phenomenon is proved to be posture dependent and associated with instability [22,23].

1.2.2. Endplates and subchondral bone

Since the endplate serves as a connection between the bone and the avascular disc material, its role is crucial in nutrition. Rajasekaran et al. marked the endplate as a hallmark of degeneration, because damage to the endplate may alter both the mechanical environment and also the nutritional pathways [24]. The thickening of the chondral endplate leads to reduction in resistance to loads and compressing forces.

The accumulating harms caused by microdamage result in the disruption of the endplate continuity. Finite element modelling (FEM), microscopic and diffusion MRI studies confirmed that cracks and breaks in endplate surfaces are the beginning of failure [25–27]. Further harms thicken the cartilage and reduce the number of blood vessels leading to further degeneration. Consequently, altered nutrition and matrix synthesis and secondary annular damage may develop [3,28]. Six stages of degeneration can be

differentiated from healthy to end-stage degeneration based on the continuity of the cartilage and presence of subchondral changes according to Rajasekaran et al. (detailed in paragraph *3.2.2. Analysis of degenerative phenotypes on MRI*)[24]. Subchondral and bone marrow changes were observed and described by Modic et al. in the late 80s. The three-grade Modic scale is still useful to detect the possible cause of back pain [20]. The factors behind bone marrow changes are still unclear, but it is closely related to mechanical insult. Altered loads affect the microenvironment of the bone marrow leading to histological changes [29]. These changes present as different signal intensities on T2-and T1-WI series. The cumulative trauma leads to oedema and micro vascularisation (Modic I., increased intensity in T1/T2 WI). As the degeneration progresses, the presence of yellow marrow in vertebral bodies can be detected (Modic II., increased on T1-WI and iso/ hyperintense on T2-WI). At the end stage woven bone formation along with the absence of yellow marrow can be seen (Modic III, decreased T1/T2 WI) [30].

1.3. Segmental instability and stenosis of the neuroforamen

Ongoing degeneration of IVD in the level of a spinal unit is presented as altered functionality. According to the degenerative cascade, the first phase is dysfunction which is characterised by the absence of osseous lesions and non-specific low back pain due to impaired restraint and muscles control. In the instability phase, abnormal movements and alignment develop due to the facet arthrosis, disc height reduction and ligamentous impairment. The altered movements usually start in the intervertebral disc, extend to the facet joints and adjacent segments, leading to segmental dysfunction and instability [31]. Segmental instability can be described as the inability to maintain biomechanical function and anatomical alignment of the involved spinal level [23]. Degenerative instability is a common cause of axial and radicular pain and consequential disability.

Intervertebral disc height narrowing leads to facet joint subluxation and reduced cranio-caudal diameter of the neuroforamen. Due to the subluxation, apical collision and sclerosis develop between the superior articular process and the overlaying superior pars interarticularis. As a result, bone remodelling, cartilage erosion of the superior process and osteophyte overgrowth may occur. This process reduces the diameter of the

foramen more and more over time. Chronic facet overload induces neocyst formation, which may extend into the foramen and/or spinal canal, compressing neural elements. [32]

The third and the last phase of the cascade is restabilisation, where significant disc collapse is associated with the formation of claw osteophytes of the vertebral body, “wrap-around bumper osteophytes” of the facet joint, as well as endplate sclerosis and vacuum phenomenon in intradiscal space [31,33].

1.4. Sagittal balance of the spine

The human spine consists of three main curves, which are essential for upright posture and bipedal walk. Aligned posture and dynamic sagittal balance are required for every day activity. Significant majority of spinal disorders are also related to the change of regional alignment and global balance. The intervertebral disc degeneration itself results in the loss of segmental lordosis (i.e., degeneration/aging increases kyphosis in general). Many studies aimed to assess and measure spinal balance via various parameters. Conventional imaging of the spine such as magnetic resonance imaging (MRI) or computer tomography (CT), are not suitable because of the lying position during the measurements. Standard full spine X-rays and/or low-dose 3D EOS™ imaging are essential to determine parameters that measure sagittal balance in standing position. There are several pelvic-, spinal and global parameters to be considered before spinal interventions.

1.4.1. Pelvic parameters

The most important base parameter is pelvic incidence (PI), which was described by Legaye [34] and Duval-Beaupère [35]. PI is the angle between the line perpendicular to the sacral plateau at the center and the line between the femoral head center and the center of the sacral plateau. It is an anatomical parameter which not only is considered constant due to its’ independency from pelvic position but it is also unique for each individual and not related to aging after growth is completed. Low PI corresponds with narrow, high PI with wide anteroposterior pelvic dimensions [36].

Sacral slope (SS) is defined as the angle between the sacral plateau and the horizontal plane. It corresponds to the position of the sacrum, where low value represents vertical, while high value represents horizontal sacral position.

DOI:10.14753/SE.2022.2689

Pelvic tilt (PT) is the angle between the line which connects the center of the sacral plateau and the femoral head center and the vertical plane. SS and PT describe the orientation of the pelvis, as the pelvis is able to rotate around the axis of the two femoral heads with the movements of retro- and anteversion. During retroversion, the SS decreases and the PT increases, in contrast during anteversion the SS increases and the PT decreases.

All three pelvic parameters are connected. as the PI is equal to the sum of SS and PT [35]. (**Figure 3**)

PI=SS+PT

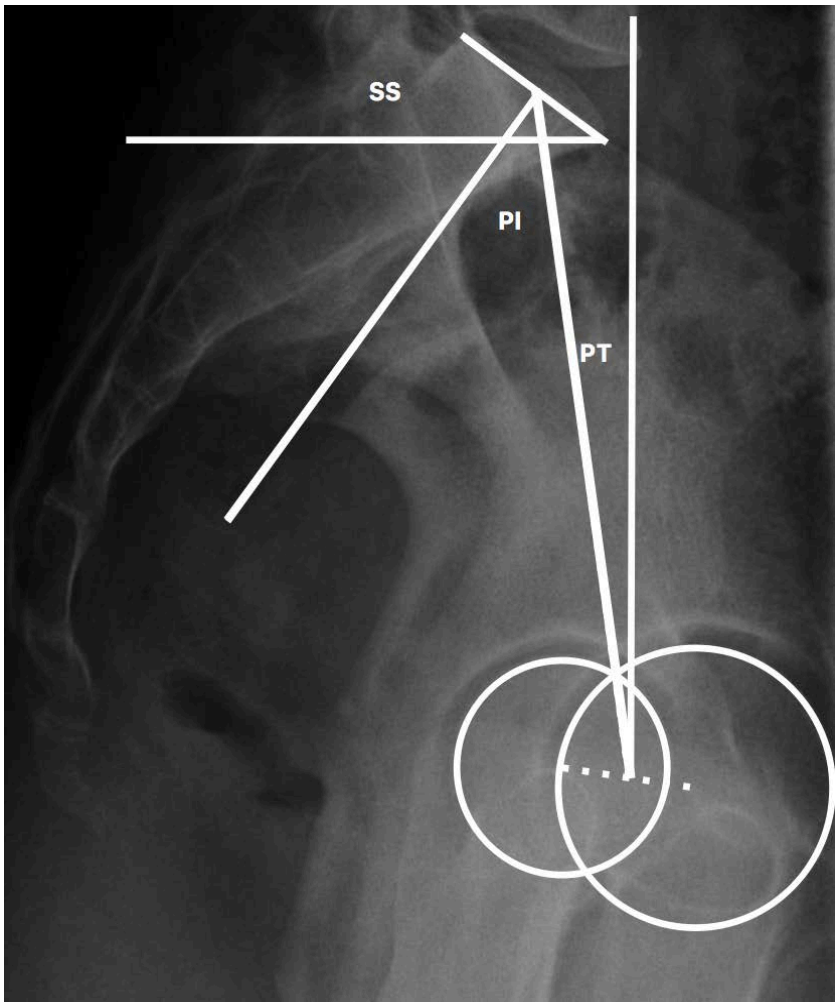

Figure 3. Pelvic parameters

Pelvic parameters shown in a lateral view X-ray SS (sacral slope), PI (pelvic incidence), PT (pelvic tilt).

1.4.2. Spinal parameters

The successive spinal curves from cranial to caudal are cervical lordosis, thoracic kyphosis and lumbar lordosis. The balanced work of spinal elements and paravertebral muscles are fundamental for upright posture. Alteration in one of these curves can influence the others and force them to compensations. Since the spine is an extremely complex structure from a biomechanical point of view, being aware of factors which influence the nature of certain mechanism is crucial. Understanding of biomechanical changes and the prediction of certain outcomes after spinal fusions are in the focus of current research. Several authors introduced various parameters to describe sagittal balance or even imbalance, they all agreed that each of the curves are essential to maintain sagittal balance [36–39].

The shape of the cervical spine can be lordotic, kyphotic and neutral. There are separated parts the upper and lower curvature. The upper part consists of the Occiput-C2 (cervical) angle, which is always lordotic. The average value is 15.81°± 7.15°. The lower part is measured between the lower endplate of C2 and the lower C7 endplate. The average value is 4.89°± 12.84° [36,40]. The thoracic kyphosis is measured as the angle between the upper endplate of Th1 (thoracic) endplate and the lower endplate of Th12. The average value is 41.83°± 10.44° [41].

Since the lifetime prevalence of low back pain is as high as 84%, lumbar surgeries are the most frequent operations in spine surgery [42]. Even short single-or two-level fusions require perioperative planning, as modification or manipulation of the lumbar lordosis is one of the key elements in restoring/maintaining the sagittal balance. Since it plays a fundamental role, preoperative x-ray measurements are as crucial as the preoperative MRI. Lumbar lordosis is measured as the angle between the upper endplate of L1 and S1 upper endplate. The average value is 55.8°± 10.2° [43]. As stated by Jackson et al., the two-thirds of lordosis occurs in the two bottom motion segments, in the most flexible and least rigid segments of the lumbar spine [44,45]. As a consequence, degeneration in L4-5 and L5-S1 discs leads to altered biomechanics and alignment. Since these two segments are the most frequent target of lumbar surgeries, considering its parameters are fundamental either in segmental or in the global point of view.

DOI:10.14753/SE.2022.2689

1.4.3. Segmental parameters

Functional spinal units or motion segments are the basic functional elements of the mobile spine. According to Schmorl, in each segment there are passive parts as the vertebral bodies, and active elements such as the intervertebral discs, the intervertebral foramen, the facet joints and the interspinosus and flava ligaments [7]. The fundamental motion segment consists of two adjacent vertebral bodies, that embrace the intervertebral disc. The anterior and posterior longitudinal ligaments border the disc from anterior and posterior aspects. The above-mentioned elements form the anterior column have a static role in passively distributing the axial load. The arcs of the two vertebras, the pair of facet joints and the posterior ligaments form the posterior column have a dynamic role as actively distributing the axial load. According to its' physical details every vertebra acts like a teeter totter, where the rotation point is the facet joint. This 'lifting device' grants active and passive load distribution [7]. (**Figure 4**)

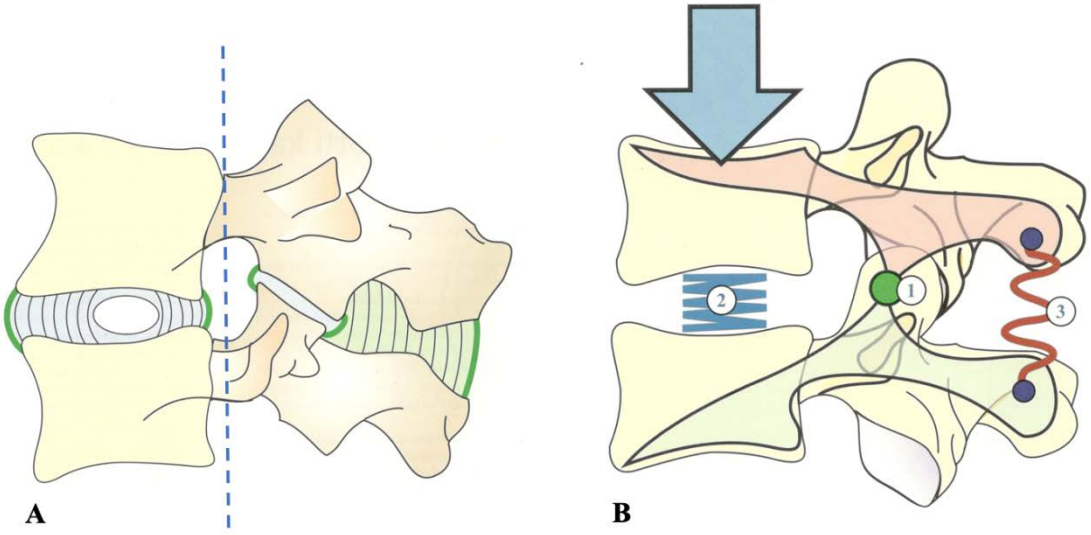

Figure 4. Structure of a motion segment

A *Elements of the anterior and posterior column.* ***B*** *Load distribution in the motion segment. (1) Axis of the movement, (2) direct passive load absorbers (IVD) (3) indirect, active load absorbers (facet joints, paravertebral muscles)[7]*

Loaded conditions can be studied on standing x-rays, via measuring various parameters to describe the condition of the two most important elements; the IVD and the neuroforamen. The physiological alignment of a lumbar segment is lordotic with a gradual increase from L1 to S1 [7]. As the aging process starts at the nucleus pulposus, the decrease of intradiscal pressure leads to disc height reduction. Anterior (DHA) and

posterior disc height (DHP) are useful parameters to follow as indirect markers of an ongoing degeneration. The changes in anterior disc height suggest an altered segmental lordosis, while the decrease in posterior disc height is a sign of foraminal stenosis. DHA and DHP also show a relationship with segmental instability factors, since disc height with advanced degeneration has a close relation with anterior vertebral slippage [22]. Dimensions of the neuroforamen in axial loaded standing X-rays, can be described by DHP and interpeduncular height (IPH). These parameters define the anterior and the cranio-caudal borders of the foramen. (**Figure 5**)

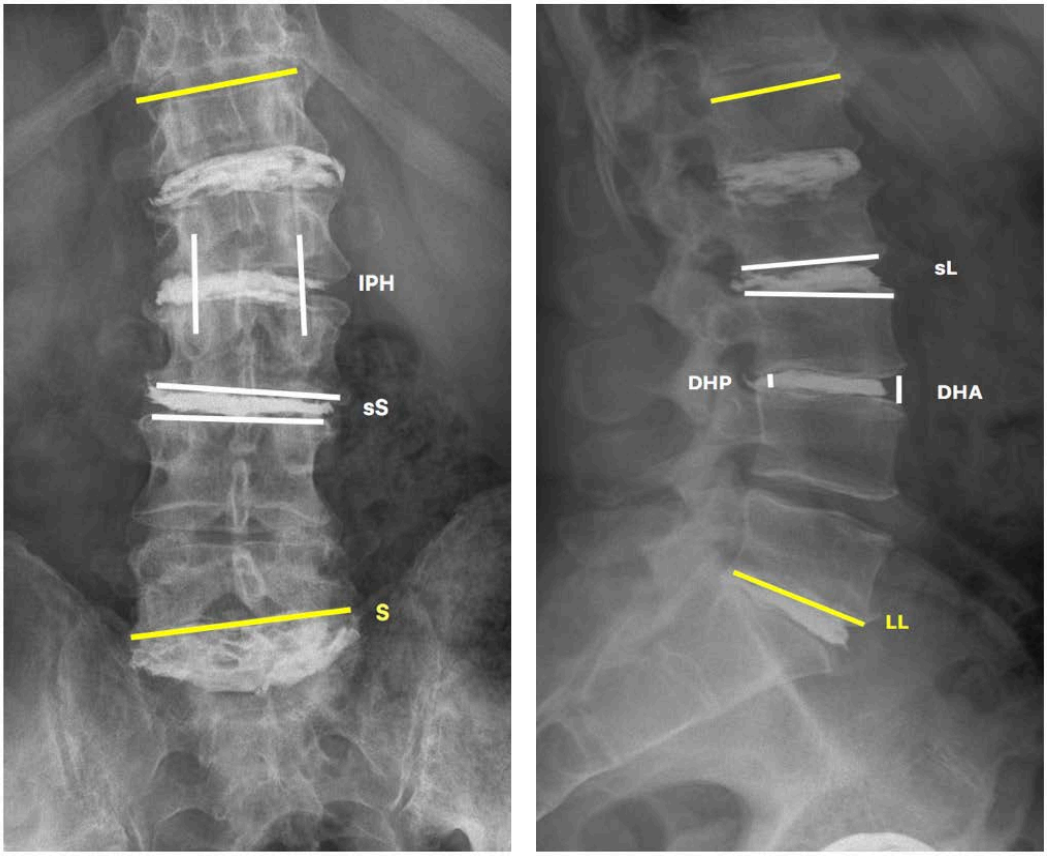

Figure 5. Spinal and segmental parameters

Spinopelvic parameters in standard standing X-ray. ***Anteroposterior view****: LS (lumbar scoliosis), sS (segmental scoliosis), IPH (interpedicular height).* ***Lateral view****: LL (lumbar lordosis), sL (segmental lordosis), DHA (disc height anterior), DHP (disc height posterior).*

1.5. Specific forms of disc degeneration

1.5.1. Advanced disc degeneration and its minimally invasive surgical treatment: the Percutaneous Cement Discoplasty (PCD)

1.5.1.1. Concept of vertical instability

As the degeneration progresses, the altered biomechanics leads to the disappearance of nucleus pulposus, total disorganisation of disc tissue and endplate sclerosis with cracks and breaks [31,33]. The intradiscal void gap in MRI or focal intradiscal hypodensity in CT is called vacuum phenomenon. This intradiscal gas is associated with disappearance of nucleus pulposus and total disc collapse. It counts as a warning sign of segmental and vertical instability [46]. In vertical instability or accordion phenomenon the height of the disc and as well as the height of neuroforamen is depending on posture [46,47]. In upright position with axial loads, low back and leg pain increase, whereas the complaints may totally diminish in lying position. These facts suggest that the cyclic vertical loading contributes to disc collapse related dynamic foraminal stenosis with nerve root and dorsal ganglia compression. In prone position, when no axial loads are applied, stenosis decreases leading to pain relief.

1.5.1.2. Percutaneous cement discoplasty – a minimally invasive treatment

The primary concept that led to the development of percutaneous cement discoplasty (PCD) was the utilisation of polymethyl-methacrylate (PMMA) as an intervertebral spacer through a transforaminal approach. Industrially preshaped spacers have a higher risk of subsidence in ageing discs with degenerated endplates [48]. The major advantage of PMMA is that it can be individually shaped, so it can easily adapt to the surface of the endplates. Varga et al. observed that PMMA fills the gaps between endplate fragments and provides an immediate stabilizing effect after hardening [47]. Ageing spine related multisegmental pathologies often require extended spinal surgeries. Longer surgeries, higher blood loss increase the morbidity rate in patients who often already suffer from various comorbidities. The more extended the surgery, the higher the risk for complications. Aiming to decrease the above mentioned risks, minimally invasive surgery (MIS) has been coming into focus to reduce the length, the blood loss of the surgery and the perioperative risks [49]. Minimally invasive percutaneous

application of stand-alone PMMA in case of vacuum discs was introduced with the conventional technique of discography. Authors named the procedure percutaneous cement discoplasty (PCD) [47]. The primary aim of PCD is to stabilise the segment in a favourable position while filling the intradiscal cavity and the gaps between the endplates [50].

1.5.1.3. Indications and contraindications of PCD

In elderly, polysegmental disc degeneration, segmental instability and consequential deformity are the leading causes of mechanical low back pain. Standing and dynamic X-rays are required to detect segmental instability and disc collapse, while CT scans are useful to assess the endplate conditions and defects, as well as vacuum phenomenon. MR imaging is required to rule out other pathologies such as infection or tumors.

Indications:

The success of this operative technique hinges on appropriate indication and patient selection.

- Elderly patients suffering from vertical instability related mechanical, axial type low back pain
- Disc collapse and vacuum phenomenon on imaging modalities
- Open procedures are contraindicated due to severe comorbidities and increased perioperative risk

Contraindications:

- Presents of tumor or ongoing infection
- Severe osteoporosis
- Motor weakness due to the severe foraminal stenosis
- Neurogenic claudication due to severe central canal stenosis
- Possibility of poor quality intraoperative images due to obesity [46,47]

1.5.1.4. Operative technique of PCD

Percutaneous cement discoplasty performed in general anaesthesia, in prone position. On a radiolucent table the intervertebral disc with the vacuum phenomenon is localised by fluoroscopy. Stab incision is made 5-7 cm laterally from the median sagittal line.

Jamshidi needle is introduced through Kambin's tringle to avoid nerve root injury. Under fluoroscopic control from lateral view, the needle is inserted into the disc space and a K-wire is inserted through the needle. After the removal of Jamshidi's tool, the vertebroplasty working channel is inserted through the K-wire, afterwards the K-wire needs to be removed. High viscosity radiopaque PMMA cement is injected into the disc space. Continuous fluoroscopic control is mandatory to observe any possible adverse event such as leakage while filling the disc space. The cement intake of the disc spaces varies in wide rage (3-10 ml). After the consolidation of the cement the work flow is removed [47]. Details of the procedure are represented in **Figure 6**. During the procedure, usually no bleeding can be observed except for the skin incision (1-2 ml).

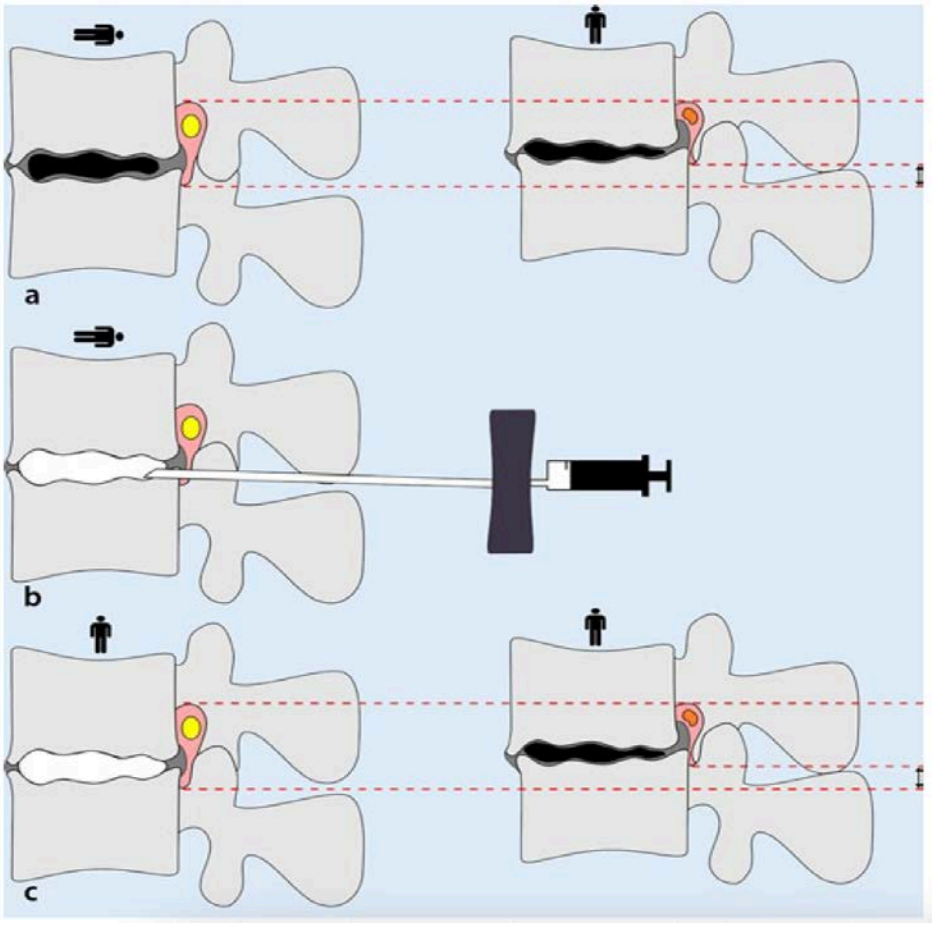

Figure 6. The concept of vertical instability and operative technique of PCD

Figure from the original article of Varga et al. [47] ***A*** *The concept of vertical instability: under axial loads, in standing position the dimensions of the neuroforamen decreases compared to lying position with*

no axial loads. ***B*** *During discoplasty the intradiscal cavity is filled with PMMA, stabilizing the segmental position with increased dimensions of the neuroforamen* ***C*** *After discoplasty the height of the foramen remains increased compared to the preoperative state*

Although the application of this technique started to spread worldwide, the number of published papers are limited to pilot studies and technical notes. Only a few studies analysed the clinical effects and consequences of PCD either in lumbar alignment or in involved segments.

1.5.2. Adjacent segment degeneration (ASD)

1.5.2.1 Incidence of ASD after lumbar fusion

Spinal fusion surgeries have become the most frequent surgical treatments in cases with degenerative disc disease and spinal instability [51,52]. Albeit, applied lumbar fusions provide stability, at the same time it limits the physiological movements of the segment, which leads to altered biomechanics in the adjacent motion segments.

The motion increases in the adjacent mobile segments, producing altered loads on facet joints and discs [53]. As a result, the reactive stabilisation process accelerates the natural ageing of the disc, resulting into adjacent segment degeneration (ASD), which was proved by Ekman et al. in a randomized controlled trial with long term follow up [54]. As ASD is a caused by accelerated ageing, it is often described by multimodal imaging such as X-rays and MRI. Radiological appearance of degeneration (ASDeg) is described by reduction of disc height, change in segmental lordosis and antero-posterior translation on X-ray [55–57]. On MRI, Disc degeneration is classified according to Pfirrmann grade [19] and consequent degenerative changes such as disc bulging, herniation, spinal canal stenosis, degenerative spondylolisthesis can develop as a result of ASD. Radiological adjacent degenerations associated with clinical symptoms called adjacent segment disease (ASDis).

The incidence of ASD varies widely in the scientific literature, where the range of ASDeg ranges between 4.8-100% with a pooled incidence of 5.9%/year [58], and the ASDis varies between 0-30.2%, with the pooled incidence of 1.8% yearly, respectively [54,58–66]. The incidence of ASDeg/ASDis related subsequent surgeries varies between 2.6-27.2% [57,62,65,67–70].

1.5.2.2 Risk factors of ASD

Identifying predisposing factors are essential to reduce occurrence, since degeneration in adjacent segments (ASD) is a major long-term complication after instrumented lumbar surgeries and the main cause of subsequent surgeries (67). The factors that influence and trigger changes in the adjacent mobile segments are currently under investigation. The factors could be classified as demographic, surgical, and pre- and postoperative radiological factors. Although the published original studies are lacking high quality evidence (average evidence: level III), a well-designed systematic review

and meta-analysis highlights the most relevant factors to consider (68). Three meta-analyses were published in the last five years, analysing the influencing factors in the lumbar spine. Phan et al. included eight studies, focused on the relationship between the ASD and spinopelvic parameters [73]. The analysis of Wang et al. consists of 19 papers, including various demographic factors, patient reported outcome measures (PROM) and spinopelvic parameters [74]. Lau et al. published a systematic review and meta-analysis, based on 16 studies including eleven risk factors [72].

In regard of demographic parameters, only body mass index (BMI) proved to be a risk factor [72,74,75]. Obesity acts like an axial overload, like carrying weights, that permanently increases the intradiscal pressure. Increased stress on dorsal components of the segment leads to degeneration [11,67]. Age is a controversial parameter, since some papers found minor impact on ASD [74] with low hazard ratios, so its clinical relevance is still questionable [68,76]. Wang et al. and Bagheri et al. introduced facet joint violation (screw placement 1 mm within the joints' edge) as a risk factor of ASD, as any violation of the stabilizing structures results in degeneration[72,74,75]. The role of preoperative spinopelvic factors remains controversial due to their moderate heterogeneity in the logistic models. Phan et al. reported, that high preoperative pelvic tilt, and high Pelvic incidence- Lumbar Lordosis mismatch (PI-LL) were risk factors of developing ASD [73]. Lau et al. found that lower preoperative LL caused anteriorly moved gravity line, which had an impact on affected discs leading to future symptoms [72,77]. These findings suggested that appropriate correction of lumbar lordosis might reduce the risk of ASD [72]. Several analyses confirmed that Pfirrmann grade 3 or higher disc degenerations were preoperative risk factors of adjacent degeneration [58,68,72,74,78–80].

The three meta-analyses suggested that certain postoperative spinopelvic parameters are risk factors of ASD. Alteration of these parameters showed an association with ASD [72]. Senteler et al. found that PI-LL mismatch greater than 15° could be predictive for revision surgeries, since PI-LL mismatch is a descriptor of pelvic morphology and lumbar alignment [81,82]. In the original paper of Schwab et al. PI-LL mismatch greater than 10° suggested sagittal malalignment [83], indicating that lordosis is not appropriate. If lumbar lordosis was less than optimal, compensatory mechanisms

modified the orientation of the pelvis resulting in alteration in spinopelvic parameters, increasing the risk of ASD.

Although various studies identified numerous risk factors, the literature lacks of well-designed prospective studies. Moreover, most studies have focused on rather rare, long stabilization surgeries and studied the development of ASD from one or few aspects despite the fact that ASD is a multifactorial, multidimensional condition.

DOI:10.14753/SE.2022.2689

2. Objectives

The aim of my PhD work was to study the above mentioned specific forms of intervertebral disc degeneration and their biomechanical and clinical aspects via three different scientific projects:

2.1. Relationship between the change of segmental and regional biomechanics and the clinical effects after percutaneous cement discoplasty

In the first section, I aimed to study a minimally invasive percutaneous technique (PCD) developed by our institution from clinical and radiological point of view. The specific research questions in this study were:

1. Does PCD lead to significant pain relief and increase in functional capacity?
2. Does this technique have an impact on the radiologic characteristics in the motion segment?
3. Does PCD influence the lumbar alignment?
4. Is any of the spinopelvic radiologic parameters associated with the clinical outcome?

2.2. In silico analysis of indirect decompression after PCD

In the second section, the effect of PMMA on neuroforaminal dimensions has been investigated applying in silico biomechanical methods. ’The following questions were investigated:

1. How does the injected PMMA influence the neuroforaminal dimensions comparing each side of the segment?
2. Does the operative technique, especially the side of the PMMA injection influence the volumetric change in the foramen and the PMMA distribution?

DOI:10.14753/SE.2022.2689

2.3. Incidence and risk factors of adjacent segment degeneration after short segment lumbar fusions

In the third section, factors that influence, induce or trigger degenerative changes in adjacent segments after short lumbar fusions were determined in a prospective clinical study. The study aimed to answer the following specific questions:

1. What is the incidence of ASD and what is the rate of ASD related subsequent surgery after routine, short-segment lumbar fusions?
2. Which radiological parameters differ pre- and postoperatively between ASD and non-ASD patients?
3. Do preoperative or postoperative spinopelvic parameters influence long-term outcome in connection with ASD after short segment lumbar surgeries?
4. Which preoperative MRI finding can have significant long-term effects on the development of ASD?
5. What are the main characteristics of the adjacent altered discs that required subsequent surgeries?

Contribution:

In this current thesis, in part '*Relationship between the change of segmental and regional biomechanics and the clinical effects after percutaneous cement discoplasty*' and in part '*Incidence and risk factors of adjacent segment degeneration after short segment lumbar fusions*' the study design, data acquisition, statistical analysis, interpretation of data and manuscript writing was done by myself under the guidance of Áron Lazáry. In part '*In silico analysis of indirect decompression after PCD'*, I was equally contributed co-author of Péter Endre Éltes, as the second investigator in measurements. **Figure 8** and **9** were created by the permission and guidance of Péter Endre Éltes.[84]

DOI:10.14753/SE.2022.2689

3. Materials and methods

All of the studies were approved by the National Ethics Committee of Hungary, the National Institute of Pharmacy and Nutrition (reference number: OGYÉI/163-4/2019). Patients participating in the study were informed and their written consents were collected.

3.1. Study cohorts and timeline

3.1.1. Percutaneous cement discoplasty: effect on radiological parameters and clinical outcome

In this retrospective analysis of prospectively collected data, data of sixty-three consecutive patients operated with percutaneous cement discoplasty technique in our tertiary care spine referral center between 2014 and 2016 were analysed. Patients with incomplete dataset (n=4), any other concomitant open surgeries (recalibration, nerve root decompression, fusion in adjacent spinal levels, (n=11) or procedures performed outside of segments L1-5 (n=17) were excluded from the study cohort. Patients required subsequent surgeries due to intraoperative complications were excluded from the cohort. (**Figure 6**) The complications were collected and classified according to Clavien-Dindo classification system (detailed in paragraph *4.1 Percutaneous cement discoplasty: effect on radiological parameters and clinical outcome*) (**Table 2**.).

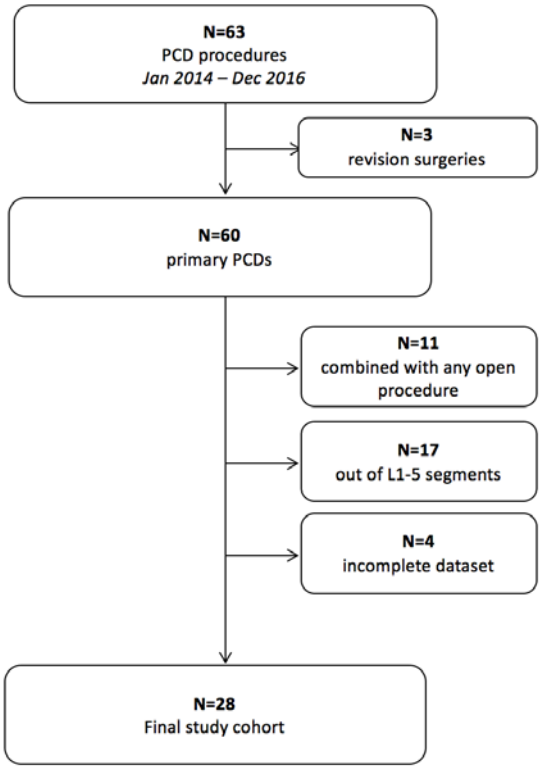

Figure 7. Study population of patients underwent percutaneous cement discoplasty

3.1.1.1. Data collection

Data were collected pre-, and postoperatively and at 6-months-follow-up. Lumbar anteroposterior and lateral standing X-rays were taken at all timepoints. Pain intensity and disability were assessed via the validated Hungarian version of Oswestry Disability Index (ODI) and the Visual Analogue Scale (VAS) preoperatively and at the follow-up.

3.1.2. In silico analysis of discoplasty

In this in silico study, radiologic and clinical data of ten patients who underwent single- or multilevel PCD were analysed. Preoperative and 6 months' postoperative data were processed.

3.1.2.1 Data collection

Pre- and 6-month postoperative CT images were taken with a predefined protocol.

3.1.3. Adjacent segment degeneration after short segment lumbar fusions

In this prospective cross-sectional study, one hundred patients, who underwent short segment lumbar transforaminal interbody fusion (TLIF) procedures due to lumbar degenerative (L1 to S1) condition were enrolled between January and May 2015. Patients were over eighteen years of age. Excluded pathologies were trauma, tumor, infection and congenital deformities. Fifteen patients were excluded from the final analysis due to incomplete dataset or surgical site infection. (**Figure 7**)

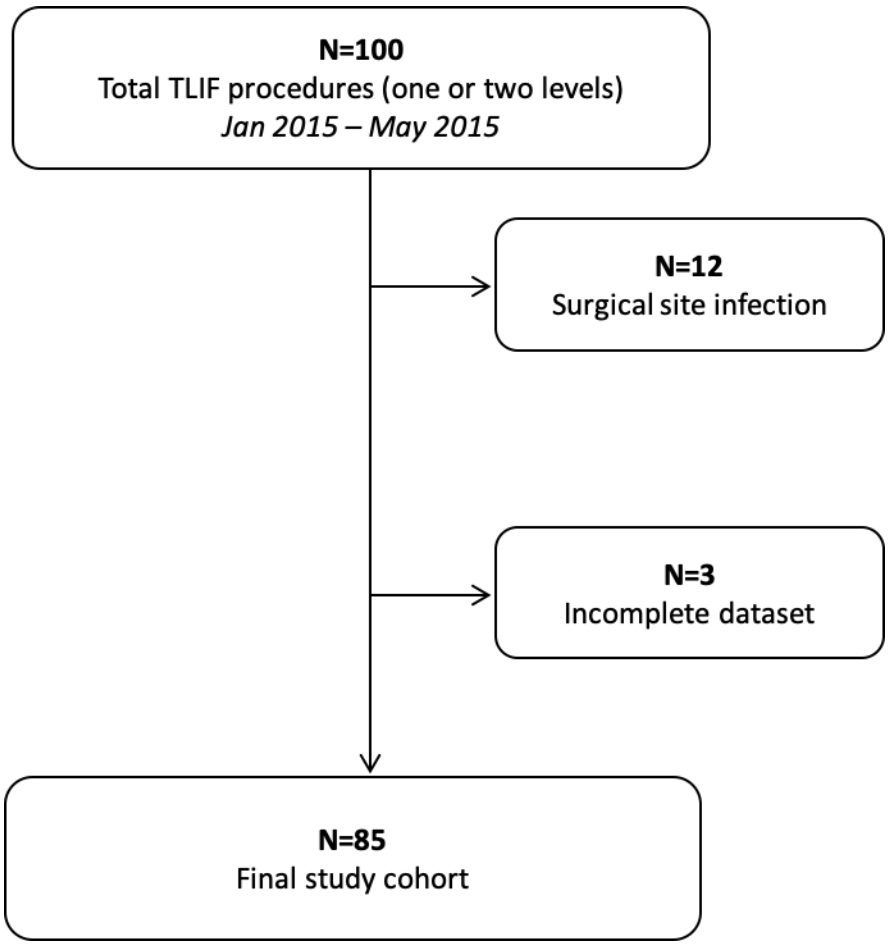

Figure 8. Study population of patients underwent short segment transforaminal lumbar interbody fusions

3.1.3.1. Data collection

The study consists of three measurement points: preoperative data, postoperative data and endpoint data. Preoperatively, standing antero-posterior and lateral X-rays and lumbar MRI were conducted within 3 months before the index surgery. Prior to the

surgery measurements of disability and pain were completed by each patients using the validated Hungarian version of Oswestry Disability Index and Visual Analogue Scale. 2-3 days after the index surgery, postoperative antero-posterior and lateral X-rays were carried out. Study endpoint was defined as 5-year follow-up after the index surgery or the time of a subsequent surgery because of ASD.

3.1.3.2. Operative technique of Transforaminal lumbar interbody fusion (TLIF)

Transforaminal lumbar interbody fusion is performed in general anaesthesia, in prone position to support lordosis of the lumbar spine. The vertical midline incision in the index level is followed by gentle retraction of skin, muscles, and soft tissues in both sides to expose the spinous process, the lamina, and the facet joints. In most of the cases unilateral foraminectomy (laminotomy and partial facetectomy) is performed. The side of the foraminectomy depends on the patients' symptoms and pathology. When the sufficient decompression is made and the liberation of the thecal sac and nerve root has been performed, the disc space can be distracted by an intralaminar spreading device. Distraction allows clear visualisation of the neural elements and the dorsal surface of the intervertebral disc. After the removal of the disc and cartilaginous endplate tissue a "banana" shaped interbody device of appropriate size is placed while retracting and protecting the dura. The interbody space then is filled with autologous/artificial bone graft posterior to the cage. Pedicle screws are placed in a standard fashion, and then attached to a lordotic rod and carefully compressed to restore lumbar lordosis while maintaining the restored disc height. The contralateral facet joint is decorticated and the bone graft is placed over for posterolateral fusion. Finally. a standard closure of layers is performed. [85,86]

3.2. Radiological measurements

Radiological measurements could be separated into two main groups based on the modality; X-ray and magnetic resonance imaging (MRI). Measurements were performed with eRad PACS viewer version 7.2 (eRAD Inc., Greenville US) and Surgimap software (Surgimap ver. 2.3.2., New York, NY).

3.2.1. Measurements of spinopelvic parameters on standing X-ray images

In all cases X-ray measurements were conducted in standing antero-posterior and lateral positions in both studies in predefined time points. Preoperative X-rays were performed within 3 months before the index surgery, while postoperative X-rays were carried out within 5 days after surgery. The follow-up/endpoint images were done at the above mentioned predefined timepoints for each study. The accuracy of the X-ray measurements was tested and determined by intrarater reliability, as the subset of cases were remeasured after two months' interval.

3.2.1.1 Spinopelvic parameters

3.2.1.1.1 Coronal plane

Lumbar scoliosis was measured according to Cobb technique, defined as the angle between upper endplate of L1 and upper endplate of sacrum. *Segmental scoliosis* is the angle between the lower endplates of superior vertebra and the upper endplate of the inferior vertebra of each motion segments. (**Figure 3**)

3.2.1.1.2 Sagittal plane

Pelvis and lumbar spine

Pelvic parameters are key factors to determine the position of the pelvis which influences the spinal curves. *Pelvic incidence* (PI) is the angle between the perpendicular drawn from the center of the S1 endplate and the line that joins the center of the femoral heads to the center of the S1 endplate. *Sacral slope* (SS) is the angle between the sacral plateau and the horizontal plane. *Pelvic tilt* (PT) is the angle between the line driven from the line that joins the two femoral heads to the center of S1 endplate and the vertical line through the center of the femoral heads (**Figure 1**). *Lumbar lordosis* (LL) is measured according to Cobb's technique, defined as the angle of the plane of the S1 and the L1 superior endplate. *Lordosis LIV-SI* (LL4S1) is angle between the plane of the S1 and the L4 superior endplate. *Segmental lordosis* is the angle between the lower endplates of the superior vertebra and the upper endplate of the inferior vertebra of each motion segment. Anterior and posterior *disc heights* (DHA, DHP) are the distances between the adjacent endplates, in the plain of the anterior/posterior vertebral borders in each motion segments. *Interpedicular height* (IPH) is defined by the distance between the centers of the adjacent pedicles and it is

used to follow the change of the height of the foramen. Mean IPH of each level from L1 to L5 was analysed (**Figure 3**).

Segmental lordosis in fusion site (sLoF) is measured as the angle between the upper endplate of the most cranial vertebra and the lower endplate of the most caudal vertebra of the fusion. If the fusion involved the sacrum, the sacral plateau is considered as the lower plane.

Measurements of adjacent segment degeneration

The main parameters to measure changes in adjacent segments were *segmental lordosis in adjacent segments, anterior/posterior disc height, and antero-posterior translation. Segmental lordosis in adjacent segments* (sL) are the angles between the upper endplates of superior vertebra and the lower endplates of the inferior vertebra of the adjacent motion segments. The *antero-posterior translation* measured as the distance between the posterior walls of the two adjacent vertebral bodies, whereas the inferior vertebra considered as fix point.

Definition of adjacent segment degeneration

ASD is determined as a radiological change between postoperative and endpoint X-rays or/and the need of surgical procedure due to degenerative pathology in the spinal segment adjacent to the index fusion [87,88]. Radiological ASD is present if at least one of the following is found on standing X-rays: (I.) onset of segmental change (either kyphotic or lordotic) equal or greater than 5°, (II.) decrease in disc height by 50 percent, (III.) anteroposterior translation equal or greater than 3 mm [55–57].

3.2.2. Analysis of degenerative phenotypes on MRI

Detailed structure analysis was performed to identify the condition of the adjacent intervertebral disc on preoperative MRIs. Five main phenotypes were studied: (1) Disc degeneration, (2) Disc bulge/protrusion and herniation, (3) Endplate damage, (4) Annular fissure, and (5) Modic changes.

(1) Disc degeneration: the distinction among the nucleus pulposus and annulus fibrosus in T2-WI MRI sequences are the base of the five-grade Pfirrmann system. In Grade I the disc shows a uniform high signal intensity on T2-WI. In Grade II, central horizontal line appears in the disc with low signal intensity. Grade III represents high

signal intensity in central nucleus, with a decreased signal in peripheral regions. Grade IV indicates blurring distinction between the annulus and the nucleus with low signal intensity. In Grade V, low and homogenous signal intensity can be seen, where the annulus and the nucleus could not be differentiated [19].

(2) Disc bulge/protrusion and herniation: displacement of disc tissue beyond the borders intervertebral disc space may be classified as diffuse (bulging) or focal (protrusion or herniation) changes. Bulging is defined as the disc material extending beyond the edges of the adjacent vertebral bodies, more than 25 percent of its circumference. A focal displacement classified as protrusion, is characterised by the disc tissue extending beyond the margin of the disc involving less than 25% of its circumference. A focal displacement is classified as herniation, if the displacement of the disc tissues appear through an annular disruption [89].

(3) Endplate damage: a trackable marker of disc degeneration process, which is classified based on its severity. The six-type-classification distinguishes between healthy (Type I), ageing (Type II-III) and degenerated (Type IV-VI) conditions. Type I is a healthy endplate; type II is a thinner endplate layer without breaks; type III is showing focal defects with no subchondral bone changes; type IV defects are visible involving less than 25% of the endplate with bone marrow changes; type V covers 50% or more surface defects with associated bone marrow changes; type VI represents damage involving almost the entire end plate [28].

(4) Annular fissures: avulsions of annular fibres and fluid tracking through the annulus fibrosus fissure presented as high signal intensity on T2-WI sequences. Presence of the annular fissure indicates morphologic changes in the annular structure without displacement of the fibrosus material [30,89].

(5) Modic change: classification of degenerative bone marrow changes was performed according to Modic et al. There are three main forms of changes involving adjacent vertebral bone marrow. Type 1 changes correspond to bone marrow oedema with a decreased signal intensity on T1-WI and increased on T2-WI. Type 2 changes reflect the yellow bone marrow in vertebral bodies with signal intensity on either T1-WI and T2-WI. Type 3 represents dens woven bone with the absence of bone marrow [20].

In further analysis all the above listed MRI parameters were dichotomized according to the following: Pfirrmann grade III or higher disc degeneration; presence of disc

bulge/protrusion or herniation; Type II or higher endplate defect; presence of annular fissure and any Modic type degeneration were considered as degenerative conditions [20,30].

Pfirrmann grade III or higher disc degeneration and/or presence of disc bulge/protrusion or herniation were considered as major degenerative sign.

3.2.3. CT acquisition

Quantitative computer tomography (CT) images were acquired from patients included in the 'In silico analysis of discoplasty' study. Pre- and 6-month postoperative images were taken applying inline calibration phantom with a previously defined protocol (MySpine study, ICT-2009.5.3 VPH, Project ID: 269909). Voxel size of the reconstructed images were 0.6x0.6x0.6 mm^3. DICOM file format exported from the hospital PACS system and anonymized via Clinical Trial Processor software (Radiological Society of North America, https://www.rsna.org/ctp.aspx) [90].

3.3. In silico measurements

In silico measurements were carried out as it was previously published by our research group [84].

3.3.1. Motion segment geometry

Segmentation process was performed applying 2D CT images, to create 3D vertebral geometry of the motion segment and the implanted PMMA spacer.[91] Manual segmentation was performed in Mimics® software (Mimics Research, Mimics Innovation Suite v21.0, Materialise, Leuven, Belgium). During the segmentation process, Hounsfield Units (HU) based thresholding provide the separation of bony volume from its' surroundings. After defining the vertebral borders, uniform filling was performed in each image slice, to provide a mask, which was the base of the future triangular surface mask. Surface smoothing (iteration: 6, smooth factor: 0,7, with shrinkage compensation) and uniform remeshing (target triangle edge length 0.6 mm, sharp edge preservation, sharp edge angle 60º) were applied. The evaluation of the segmentation process was performed by the comparison of randomly selected vertebral geometries (6 preoperative, 6 postoperative measurements). Dice Similarity Index (DSI) was applied to evaluate the accuracy of the measurements [92,93]. This index defined

the relative volume overlapping between 3D objects. DSI was calculated by the following equation: $DSI=(2\cdot V(I_1 \cap I_2))/(V(I_1) + V(I_2))$, where V was the volume of the voxels inside the binary mask, and I_1 and I_2 were the binary masks from two segmentation processes of the two investigators (I). The segmentation was performed by two investigators at two different time points.

3.3.2. Alignment of the motion segments' geometry

To detect and measure the effect of discoplasty in motion segments, pre-, and postoperative vertebral body models were adjusted in a common coordinate system. These models of the same motion segment were registered applying the caudal vertebra as reference, based on 18 anatomical landmarks as predefined registration points. For the rigid registration procedure, the algorithm of Mimics® software was implemented. To evaluate the accuracy of the registration process Hausdorff Distance (HD) was measured via MeshLab1.3.2 software (http://www.meshlab.net) [94]. HD was the maximum distance between to registration points, where 0 represented the absolute perfect alignment. HD measurements were performed in all 16 segments by both investigators.

3.3.3. Measurement of the neuroforamen

After the registration of pre- and postoperative models, the effect of the PCD was shown as the displacement of the cranial vertebra, which led to change in either in the spinal canal or in the neuroforamen geometry. This alteration was measured by a cylinder inserted in the virtual coronal axis of the neuroforamen. The length of the cylinder was predefined by 90 mm, but the radius was adjusted individually for each segment, to exceed the bony borders of the neuroforamen and central canal. The overlapping volumes were substracted from the cylinder. The change in volumes represented the dimensions of the neuroforamen and the canal either pre- and postoperatively. The changes in substracted volumes ($\Delta V=V_{postop}-V_{preop}$) represented the effect of the surgery, the volumetric alteration of indirect decompression. The measurement defined the quantitative effect of indirect decompression in the whole spinal unit. (**Figure 8**) To determine changes in more details, left and right side changes have been analysed separately. A uniform cutting plane was inserted into each motion

segment in the median sagittal plane, which defines the left and right neuroforamen as a cropped cylinder and even the volumetric distribution of PMMA. (**Figure 9**)

The accuracy and repeatability of the measurement was evaluated by intrarater reliability between the investigators and in two time points, respectively.

DOI:10.14753/SE.2022.2689

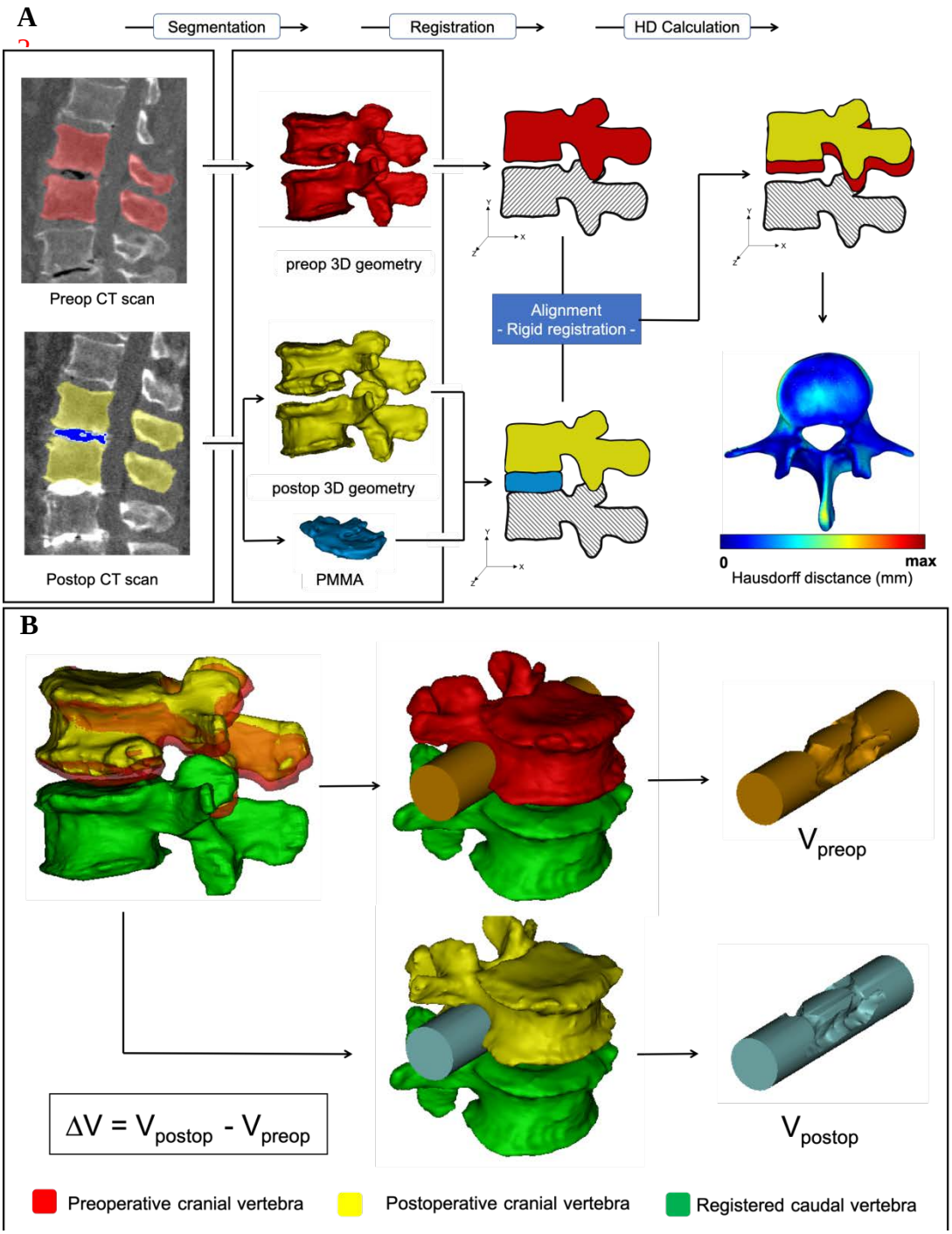

Figure 9. Process of segmentation, registration and measurements of cylinder volume *[84]84*

A) Manual segmentation of 2D CT images to produce 3D volume of the coloured masks of the vertebra and PMMA. Rigid registration of the 3D volumes based on predefined anatomical points, which provided a common coordinate system for preop and postop models. Hausdorff distance was used for a quality measurement of the rigid registration. **B** As the pre- and postoperative measurements aligned in the same coordinate system, the effect PCD resulted in change of the position of the cranial vertebra. In both pre-and postop. Motion segments, two identical cylinders were inserted into the central canal and the neuroforamen. Overlapping

surfaces were substracted from the cylinder volume (V preop and V postop). The indirect decompression effect of PCD represented by ΔV=Vpostop-Vpreop.

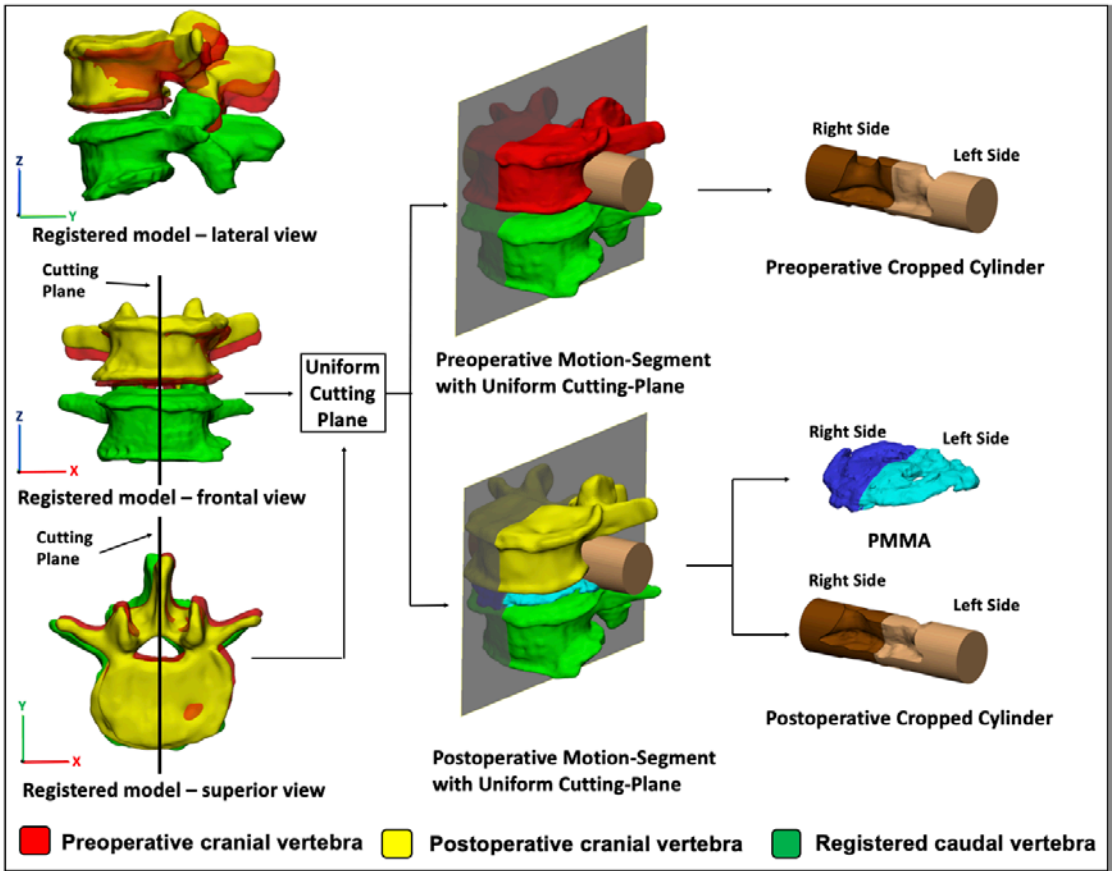

Figure 10. Application of a uniform cutting plane *[84]*

3.4. Patient reported outcome measures

Patient-reported outcome measures (PROMs) assess the person's perception of their current health status via self-reported questionnaires. Outcome measures enable subjects to report on their daily functioning, symptoms and other aspects of their health and well-being. Health care can gain objective feedback of changes in quality of life and disability after certain treatments using pre-, and post-therapy surveys. In this study the Hungarian version of Oswestry Disability Index (ODI) and Visual Analogue Scale were applied to assess subjects' health status preoperatively and at the follow-up.

3.4.1. Oswestry Disability Index (ODI)

This questionnaire was first published in 1980 by O'Brien and Fairbank. [95] Since its first appearance several changes were applied over time. The ODI was translated and

validated on more than ten languages, including the Hungarian version by Valasek et al [96]. The current valid English version is 2.1b, but the base of the all the current foreign version were version 2.1a. The questionnaire consists of ten subdivisions including pain intensity, personal care, lifting, walking, sitting, standing, sleeping, sex life, social life and traveling. For each subdivision, there are six statements, from the best to the worst choice scored from 0 to 5. The formula for calculating the score is the total achieved score divided by the maximum achievable score and the result multiplied by 100. The score rages on a scale from 0 to 100, where the higher the score the higher the disability. According to the questionnaire developers, the result is valid if at least 9 questions are answered [95].

3.4.2. Visual Analogue Scale (VAS)

A Visual Analogue Scale (VAS) is an instrument that is designed to measure a characteristic or attitude that is believed to range across a continuum of values and cannot be directly measured. VAS is a horizontal line 100 mm in length, marked by word descriptors at start and at end. The subject marks the line in a certain point that represents their current state. The VAS score is determined by measuring in millimetres from the left-hand end of the line to the point that the patient marks [97]. In our particular study VAS was used to measure pain intensity, where higher scores represented higher pain intensity.

Patient marked the line answering the following question about low back and leg pain:

"How severe was your back pain in the last week?"

"How severe was your leg pain (sciatica)/buttock pain in the last week?"

3.5. Statistical analysis

3.5.1. Percutaneous cement discoplasty: effect on radiological parameters and clinical outcome

All spinopelvic parameters were measured and a randomly selected subset of 20 samples were remeasured after a two months' interval by the same investigator, to determine intraclass correlation coefficient (ICC), and to evaluate the intra-rater reliability of the measurement methods. According to the original publication of Cicchetti et al. the ICC is: less than 0.40 = poor, between 0.40-0.59 = fair, between 0.60-0.74, or more than 0.75= excellent [98]. Distribution of data was determined by the

Shapiro-Wilk test. For normally distributed variables the parametric one-way repeated measures ANOVA, for non-parametric variables the Friedman test were applied. The ANOVA and Friedman test were chosen based on the study design, as the parameters were measured multiple times (preoperative, postoperative and follow-up data) to see changes related to the surgery. Statistical significance was determined between the two groups over the course of a 6-month follow up period. If the overall ANOVA result proved significant, post hoc analysis with Bonferroni adjustment was applied to discover which specific means differed.

To measure the strength and direction of the association between the change of spinopelvic parameters and the clinical outcomes, Pearson's correlation (r) for parametric and Spearman (rho) correlation for non-parametric variables were applied. Cohen's standard was used to evaluate the strength of the relationship (r/rho between 0.1 and 0.29 represents a 'small', r/rho between 0.3 and 0.49 represents a 'medium' and r/rho above 0.5 represents a 'large' association). Statistical analyses were performed using the SPSS 20.0 software (IBM Corp., IBM SPSS Statistics software, Chicago, IL, USA). A p-value of less than 0.05 was considered significant.

3.5.2. In silico analysis of discoplasty

Due to the low number of patients in the cohort, non-parametrical tests were used to compare values. Mann-Whitney U test was applied to compare right and left sides, related-sample Wilcoxon signed rank test was carried out to compare pre-, and postop data. Spearman's rho was conducted to assess the relationship between PMMA intake and volumetric changes for each side.

3.5.3. Adjacent segment degeneration after short segment lumbar fusions

Further comparison of spinopelvic X-ray measurements between ASD and Non-ASD groups were assessed by Student's t-tests for parametric variables and Mann-Whitney U test for nonparametric variables. For categorical variables Chi-square or Fisher's exact test was applied to identify the relationship of the parameters. Statistical analysis was performed using SPSS software (IBM Corp. released 2016. IBM SPSS Statistics, Version 24.0. Armonk, NY).

Multivariate logistic regression models were built to identify which factors may affect the development of ASD. Spinopelvic and MRI phenotypes that were not distributed

equally across groups were selected. Stepwise backward conditional method was applied to extract the final model. Multicollinearity was evaluated by Pearson's rank correlation test ($r>0.8$). Statistical analysis was performed using SPSS software (IBM Corp. released 2016. IBM SPSS Statistics, Version 24.0. Armonk, NY).

DOI:10.14753/SE.2022.2689

4. Results

4.1 Percutaneous cement discoplasty: effect on radiological parameters and clinical outcome

Twenty-eight patients, with 112 segments (65 PCD and 47 without PCD) were analysed. The study cohort consisted of a quarter of males (7/28) to three-quarters of females (21/28). The extent of surgery, the number of the operated levels/cases are shown in **Table 1**.

Table 1. Characteristics of study population

N	28
Age (years, mean±SD)	75.4±7.4
Gender (M/F)	7/21
Extent of surgery (number of PCD levels)	
1 level	9 (9)
2 levels	6 (12)
3 levels	8 (24)
4 levels	5 (20)
Operating time (min, mean±SD)	
1 level	22.5±3.5
2 levels	25.0±5.0
3 levels	38.8±11.1
4 levels	64.3±12.7

Surgical complications which were excluded from the study (cement leakage, n=3) were listed and classified according to Clavien-Dindo classification. All cases were excluded from the final cohort (**Table 2**) [99].

Table 2. List of excluded complications according to Clavien-Dindo Classification

Primal surgery	Symptom	CT	Clavien-Dindo	Revision surgery

			Classification	
Percutaneous cement discoplasty L5/S1	Severe left leg pain	Cement leakage in left L5/S1 foramen	Grade IIIb	Decompression and removal of cement from left L5/S1 foramen
Percutaneous cement discoplasty L4/5 and L5/S1	Severe left leg pain	Cement leakage in left L5/S1 foramen	Grade IIIb	Decompression and removal of cement from left L5/S1 foramen
Percutaneous cement discoplasty L2/3, L3/4, L4/5 and L5/S1	Severe left leg pain	Cement leakage in left L5/S1 foramen	Grade IIIb	Decompression and removal of cement from left L5/S1 foramen

The results were reported comparing the preoperative (preop), postoperative (postop) and six months follow up (6M FU) data.

4.1.1. Pelvic parameters

The pelvic incidence was constant during the study period (preop vs. postop $p>0.05$ and post vs. 6M FU $p>0.05$). Sacral slope significantly increased after the intervention and the change remained constant (preop vs. postop $p<0.01$, postop vs. 6M FU $p>0.05$). A significant, constant decrease of pelvic tilt was observed after the PCD procedure (preop vs. postop $p<0.05$, post vs. 6M FU $p>0.05$). (**Table 3**)

Table 3. Results of radiological measurements: Pelvic parameters

	preop (mean±SD)	postop (mean±SD)	6M FU (mean±SD)	postop vs preop (mean change, %)	p	6M FU vs postop (mean change, %)	p
Pelvic parameters							
PI (°)[#]	54.5±8.9	54.7±9.5	55.2±9.6	0.2 (0.3%)	>0.05	0.5 (0.9%)	>0.05
SS (°)[#]	33.6±7.1	36.5±7.0	35.0±6.8	2.9 (8.6%)	**<0.01**	-1.5 (-4.11%)	>0.05
PT (°)[#]	21.1±10.1	18.3±8.1	19.9±9.1	-2.8 (-13.28%)	**<0.05**	1.6 (8.7%)	>0.05

PI (pelvic incidence, SS (sacral slope), PT (pelvic tilt). Pre-op vs. post-op and post-op vs. FU change percentage represented in parentheses. # Normally distributed data

4.1.2. Spinal parameters

No significant change was found in the global L1-5 lumbar lordosis after the procedure, however a 3.4° trend to significant increase in the lordosis was observed ($p>0.05$). Segmental lordosis significantly increased in both segments with and without PCD

($p<0.05$ and $p<0.05$) and the change was constant during the follow-up period. In case of all measured segments the segmental lordosis (4.4±3.8° vs. 6.6±4.8° vs. 6.9±4.7°) showed significant, constant change after the procedure ($p<0.05$). Correction of lumbar scoliosis could be achieved and maintained (7.4±6.4° vs. 5.6±5.4° vs. 5.7±6.1°). The degree of scoliosis was statistically different pre- and postoperatively ($p<0.05$) but there was no significant change after 6 months ($p>0.05$). A significant segmental deformity correction was observed after the PCD procedure without any change over the 6 months follow-up (4.7±3.7° vs. 2.4±1.9° vs. 2.5±2.1°, $p<0.05$ and $p>0.05$). (**Table 4**)

Table 4. Results of radiological measurements: Spinal parameters

	preop (mean±SD)	**postop** (mean±SD)	**6M FU** (mean±SD)	**postop vs preop** (mean change, %)	**p**	**6M FU vs postop** (mean change, %)	**p**
Spinal parameters							
LL (°)[#]	35.5±16.3	38.9±16.5	38.0±16.7	3.4 (9.5%)	>0.05	-0.9 (-2.32%)	>0.05
sL (°)	4.4±3.8	6.6±4.8	6.9±4.7	2.2 (73.6%)	*<0.05*	0.3 (4.5%)	>0.05
segments with PCD (°)	3.2±3.4	4.7±3.7	5.4±3.7	1.5 (38.2%)	*<0.05*	0.7 (14.89%)	>0.05
segments w/o PCD (°)	5.9±3.8	9.0±4.8	9.1±4.9	3.1 (136.8%)	**<0.05**	0.1 (1.1%)	>0.05
LS (°)	7.4±6.4	5.6±5.4	5.7±6.1	-1.8 (-12.5%)	**<0.05**	0.1 (1.1%)	>0.05
sS (°)	6.5±4.8	2.3±2.1	2.6±2.2	-4.2 (-52.1%)	**<0.001**	0.3 (13%)	>0.05
Segments with PCD (°)	4.7±3.7	2.4±1.9	2.5±2.1	-2.3 (-33.14%)	**<0.05**	0.1 (4.1%)	>0.05
segments w/o PCD (°)	8.8±5.0	2.2±2.3	2.6±2.3	-6.6 (-66%)	**<0.001**	0.4 (18.18%)	>0.05

LL (lumbar lordosis). LS (lumbar scoliosis), sL (segmental lordosis), sS (segmental scoliosis), Pre-op vs. post-op and post-op vs. FU change percentage represented in parentheses. # Normally distributed data

4.1.3. Intervertebral space parameters

In sagittal plane, the anterior (DHA) and posterior disc height (DHP) showed a significant increase after the surgery (DHA: 5.5±2.7mm vs. 9.1±2.8mm, p<0.001; DHP: 4.0±2.3mm vs. 5.5±2.6mm, p<0.001). In both parameters, the change was significantly higher in PCD treated segments (DHA mean change: 4.7±3.0mm vs. 2.1±3.3mm, p<0.001; DHP mean change: 2.8±3.4mm vs. 0.0±2.4mm, p<0.001 in case of segments with and without PCD, respectively). IPH significantly increased in segments with PCD and the change remained constant (28.8±3.6mm vs. 32.8±4.5mm vs. 31.7±4.6mm, p<0.001). (**Table 5**)

Table 5. Results of the radiological measurements: Intervertebral parameters

	preop (mean±SD)	**postop (mean±SD)**	**6M FU (mean±SD)**	**postop vs preop (mean change, %)**	**p**	**6M FU vs postop (mean change, %)**	**p**
DHA (mm)	5.5±2.7	9.1±3.2	8.3±3.3	3.6 (65.4%)	**<0.001**	-0.8 (-8.8%)	**<0.001**
Segments with PCD (mm)	4.5±2.1	9.2±2.8	8.4±2.9	4.7 (104.4%)	**<0.001**	-0.8 (-8.7%)	<0.05
segments w/o PCD (mm)	6.8±2.8	8.9±3.6	8.2±3.8	2.1 (30.8%)	**<0.001**	-0.7 (-7.8%)	<0.05
DHP (mm)	4.0±2.2	5.5±2.7	5.2±2.7	1.5 (37.5%)	**<0.001**	-0.3 (-5.4%)	**<0.05**
segments with PCD (mm)	4.0±2.3	6.8±2.6	6.5±2.5	2.8 (70%)	**<0.001**	-0.3 (-4.4%)	>0.05
segments w/o PCD (mm)	4.0±2.0	4.0±2.0	3.4±1.6	0.0 (0%)	>0.05	-0.6 (-15%)	***<0.05***
IPH (mm)	30.1±3.7	32.4±3.3	31.5±3.4	2.3 (7.6%)	***<0.05***	-0.9 (-2.8%)	***<0.001***
segments with PCD (mm)	28.8±3.6	32.8±4.8	31.7±4.6	4.0 (13.8%)	***<0.001***	-1.1 (-3.3%)	**<0.05**
segments w/o PCD (mm)	31.4±4.0	16.0±3.3	31.1±3.5	-15.4 (-49.1%)	>0.05	15.1 (94.3%)	>0.05

DHA (disc height anterior), DHP (disc height posterior), IPH (interpedicular height). Pre-op vs. post-op and post-op vs. FU change percentage represented in parentheses.

In case of multi-level PCDs (2 or more segments), the change of lumbar scoliosis (-2.2±3.2°) and segmental scoliosis (2.5±4.5°) showed significant difference compared to single level PCDs (change in LS= -0.7±2.4° and in sS=7.3±5.4°; $p<0.05$ and $p<0.01$ compared to multi-level PCD). The change in posterior disc height (0.2±2.9mm vs. 2.1±2.9mm, $p<0.05$) showed more increase in multi-level PCDs. (**Table 6**).

Table 6. Difference between single- and multilevel (2+) PCDs

	Levels	preop (mean±SD)	postop (mean±SD)	preop vs. postop (mean change±SD) (%)	p
Pelvic parameters					
SS(°)	Single	38.2±4.8	41±5.9	2.7±4.1 (6.8%)	
	Multi	31.4±6.4	34.4±6.9	3.0±4.9 (8.7%)	>0.05
PT(°)	Single	18.5±7.2	16.1±5.4	-2.4±4.4 (-15.2%)	
	Multi	22.3±8.7	19.3±10.8	-2.9±5.2 (-15.2%)	>0.05
Spinal parameters					
LL(°)	Single	49.4±14.1	52.7±15.9	3.3±4.8 (6.3%)	
	Multi	28.9±11.9	32.3±12.4	3.4±8.6 (10.6%)	>0.05
sL(°)	Single	5.6±4.4	9.6±4.3	4.1±5.7 (42.1%)	
	Multi	3.7±4.3	5.0±3.3	1.3±4.4 (25.7%)	**<0.05**
LS(°)	Single	5.5±4.8	4.7±5.1	-0.7±2.4 (-16.3%)	
	Multi	8.2±5.4	6.0±6.8	-2.2±3.2 (-36.5%)	**<0.05**
sS(°)	Single	9.6±4.3	2.3±2.3	7.3±5.4 (-96.6%)	
	Multi	4.9±4.2	2.3±2.0	2.5±4.5 (-110.7%)	**<0.01**
Intervertebral parameters					
DHA (mm)	Single	7.0±3.1	9.8±3.6	2.8±4.2 (28.9%)	
	Multi	4.8±2.9	8.6±2.2	3.8±2.8 (44.4%)	>0.05
DHP (mm)	Single	4.1±2.2	4.3±2.1	0.2±2.9 (5.7%)	
	Multi	3.9±2.9	6.1±2.2	2.1±2.9 (35.8%)	**<0.05**
IPH (mm)	Single	31.1±3.8	32.6±3.6	1.5±4.0 (4.6%)	
	Multi	29.5±3.0	32.1±2.8	2.6±3.1 (8.1%)	>0.05

PI (pelvic incidence), SS (sacral slope), PT (pelvic tilt), LL (lumbar lordosis). LS (lumbar scoliosis), sL (segmental lordosis), sS (segmental scoliosis), Preop vs. postop and postop changes percentage represented in brackets.

Intrareter reliability of the radiological measurements proved to be excellent based on the calculated ICC. (**Table 7**).

Table 7. Intraclass correlation coefficient of the measured parameters

Variable	ICC	95% CI
PI	*0.99*	*(0.978- 0.998)*
SS	*0.98*	*(0.951- 0.992)*
LL	*0.99*	*(0.987- 0.998)*
LS	*0.96*	*(0.925- 0.988)*
sL	*0.93*	*(0.831- 0.972)*
DHA	*0.91*	*(0.808- 0.966)*
DHP	*0.79*	*(0.553- 0.921)*
IPH	*0.98*	*(0.961- 0.994)*

4.1.4. Clinical outcome

ODI and VAS (both LP and LBP) significantly decreased 6 months after the PCD procedure (**Table 8**).

Table 8. Clinical outcome

	preop (mean±SD)	6M FU (mean±SD)	6M FU vs postop (mean change, %)	p
ODI	55.4±13.9	37.9±21.4	-37.9 (-31.5%)	**<0.001**
LBP	5.9±3.0	3.5±2.5	-3.5 (-40.6%)	**<0.001**
LP	6.9±2.4	4.0±2.7	-4.0 (-42%)	**<0.001**

ODI (Oswestry Disability Index), LBP (low back pain), LP (leg pain). Preop vs. postop and postop change percentage represented in brackets

There was a moderately strong association between the increase of sacral slope and improvement of ODI postoperatively (rho=-0.39, $p<0.05$) (**Figure 10**)

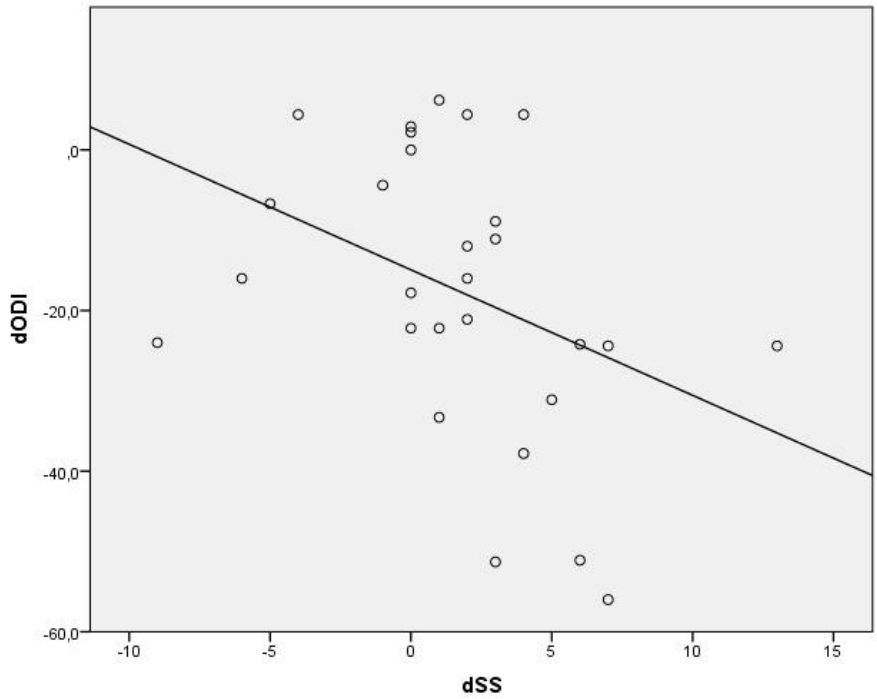

Figure 11. ***Association between the postoperative change in Sacral Slope (SS) and Oswestry Disability Index (ODI)*** *(rho=-0.39, p<0.05).*

We also found that the change of LBP was significantly correlated with the degree of segmental scoliosis correction (rho=0.32, p<0.001). There was also a weak but significant correlation between the increase of DHA and ODI (rho=-0.189, p<0.05) and between DHA and DHP and LP (rho=-0.202, p<0.05 and rho=-0.274, p<0.05, respectively). (**Table 8**)

The improvement of leg pain (-1.8±2.5 vs. -3.2±2.3, p<0.05) was significantly greater in multilevel procedures. Impact of PCD based on the number of discoplasty is presented in **Table 9**.

Table 9. Clinical outcome (single vs. multilevel)

	Levels	preop (mean±SD)	postop (mean±SD)	preop vs. postop (mean change±SD), (%)	p
ODI	Single	58.6±9.7	42.8±22.6	-15.8±20.5 (-37.0%)	>0.05
	Multi	53.8±10.1	35.5±15.1	-18.3±15.7 (-51.7%)	
LBP	Single	5.6±3.0	2.5±2.1	-3.1±3.1 (-121.5%)	>0.05
	Multi	5.9±2.6	3.8±2.9	-2.0±3.0 (-53.0%)	
LP	Single	7.5±1.9	5.6±2.0	-1.8±2.5 (-33.3%)	**<0.05**
	Multi	6.5±2.5	3.2±2.5	-3.2±2.3 (-100.3%)	

ODI (Oswestry Disability Index), LBP (low back pain), LP (leg pain). Preop vs. postop and postop change percentage represented in brackets. P-value represents the difference between single and multilevel procedures

4.2. In silico analysis of discoplasty

In the present analysis 16 segments of ten patients were included. The mean age was 74±7.7 years. The levels of the involved segments were L5-S1 (2/16, 12.5%), L4-L5 (4/16, 25%), L3-L4 (4/16, 25%), L2-L3 (2/16, 12.5%), L1-L2 (3/16, 18,5%), Th12-L1 (1/16, 6,25%). (**Figure 11**)

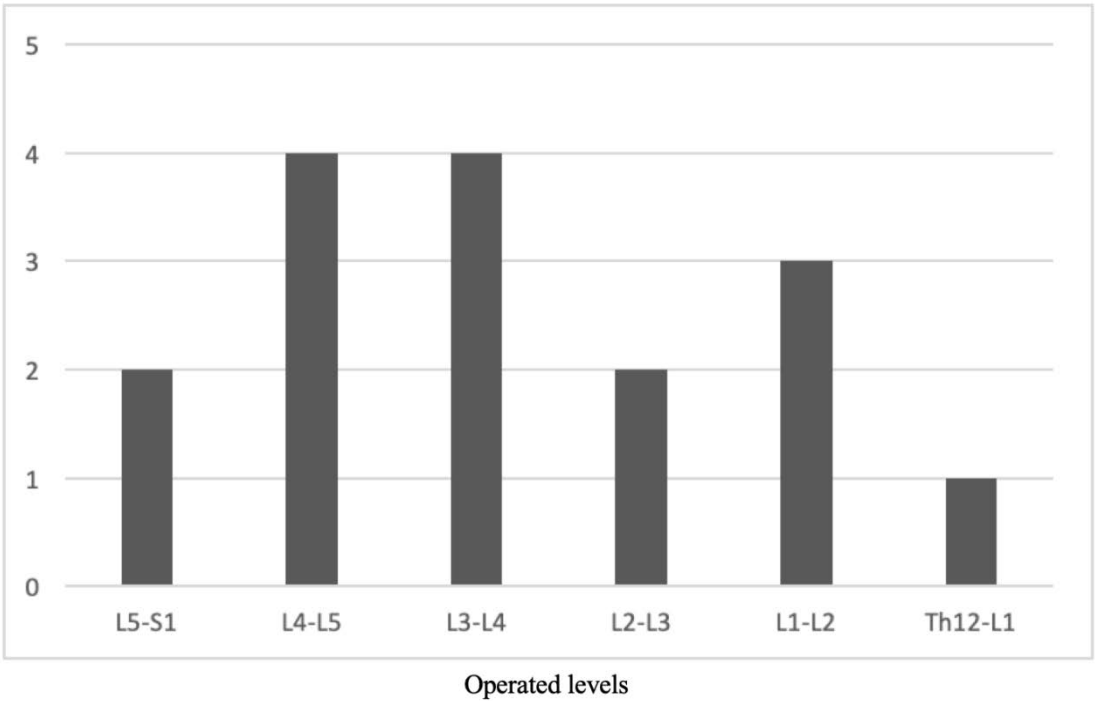

Figure 12. Number of treated segments by spinal level

There was no significant difference between right and left side either pre- (11136.69 mm^3 mm^3±3616.94 mm^3 vs. 10534.93 mm^3±2285.76 mm^3; p=0.616) or postoperatively (12184.75 mm^3±3453.64 mm^3 vs. 11701.58 mm^3±2283.32 mm^3; p=0.752). The volumetric change did not differ between the two sides (1048.06 mm^3±605.68 mm^3 vs. 1166.65 mm^3±691.01 mm^3; p=0.590). (**Figure 12**)

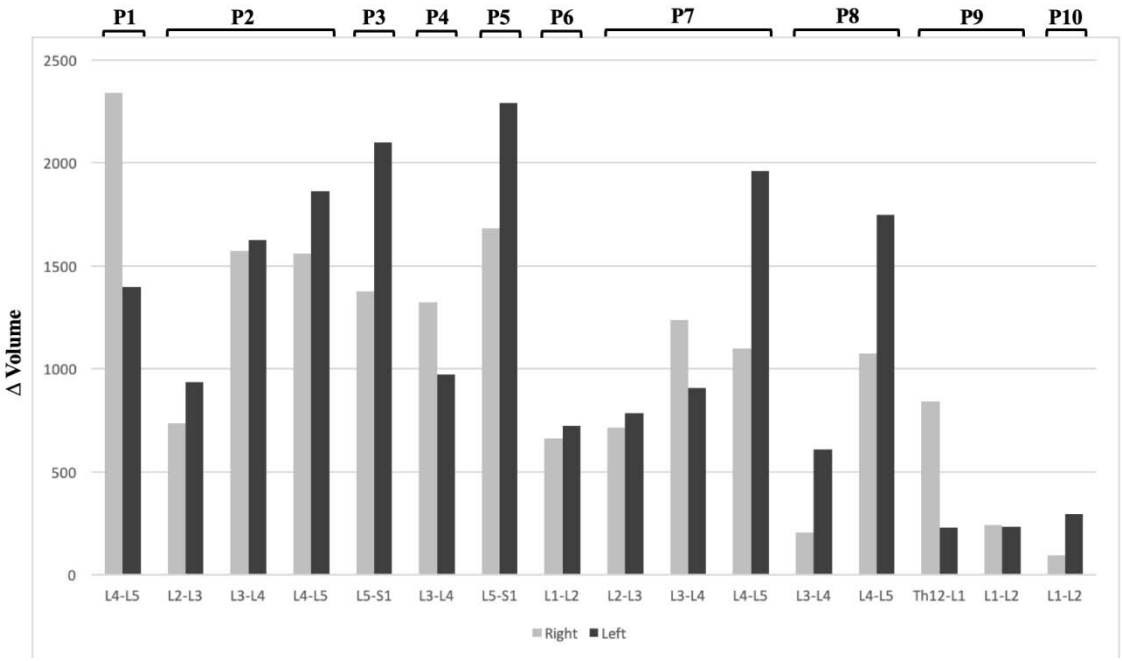

Figure 13. Volumetric change of the neuroforamen at right and left side in each segment

Axis 'x' represents the treated segment, where right and left side is shown according to the legend. 'P' represents patient. Axis 'y' presents the change in neuroforamen volume.

The postoperative cylinder volume significantly increased compared to preoperative cylinder values either right (11136.69±3616.94 vs. 12184.75±3453.64; p<0.0001) or left side (10534.93 mm^3±2285.76 mm^3 vs. 11701.58 mm^3±2283.32 mm^3; p<0.0001).
In regard of PMMA intake (3622.51mm^3±1573.42 mm^3 vs. 3981.23mm^3±2048.44 mm^3; p=0.616) and distribution (0.49%±0.17% vs. 0.51%±0.17%; p=0.985) both seemed equal, with no significant difference. The volumetric change showed a strong correlation with PMMA volume in right side (rho=0.682; p=0.004) and in left side (rho=0.650; p=0.006), *(***Table 10**, **Table 11***)*.

In regard of the side of the discoplasty, there was no difference neither in preop (11216.46 mm^3±2656.45 mm^3 vs. 10455.15 mm^3±3336.78 mm^3; p=0.361) nor in postop cylinder volumes (12318.87 mm^3±2295.41 mm^3 vs. 11567.45 mm^3±3419.88 mm^3; p=0.468) between the filling and the contralateral sides. The delta volume increase was almost equal (1102.41 mm^3±646.08 mm^3 vs. 1112.30 mm^3±659.05 mm^3; p=0.724), even the amount of injected PMMA volume (3912.19 mm^3±1756.92 mm^3 vs. 3691.54 mm^3±1904.63 mm^3; p=0.985). The injected cement distributed equally between the right and left side (0.52±0.17 vs. 0.48±0.17; p=0.696) (**Table 12**).

Table 10. Volumetric measurements on the right side

			Right (n=9)				
Patient ID	**Treated segment**	**Side of discoplasty R/L**	**Substracted cylinder volumes (preop mm3)**	**Substracted cylinder volumes (Postop mm3)**	**Delta volume (mm3)**	**PMMA volume (mm3)**	**Distribution of total PMMA (%)**
P01	L4-5	R	10571.31	12912.48	2341.16	6476.52	0.64
P02	L2-3	R	12913.27	13650.33	737.06	1786.30	0.28
	L3-4	L	14503.03	16076.10	1573.07	4715.25	0.56
	L4-5	L	8835.33	10394.26	1558.92	3427.19	0.53
P03	L5-S1	L	5031.57	6406.67	1375.09	3390.91	0.33
P04	L3-4	L	18089.48	19412.29	1322.80	2141.88	0.34
P05	L5-S1	R	7132.74	8817.247	1684.50	5637.68	0.54
P06	L1-2	R	11371.99	12034.59	662.59	1697.98	0.33
P07	L2-3	L	8557.05	9272.09	715.03	4076.39	0.67
	L3-4	L	6753.21	7990.86	1237.65	6094.34	0.64
	L4-5	R	6860.46	7961.43	1100.96	4896.51	0.51
P08	L3-4	L	13939.09	14142.29	203.20	1530.477	0.18
	L4-5	R	12853.71	13929.88	1076.17	3349.10	0.29
P09	Th12-L1	R	12666.42	13508.12	841.70	3464.11	0.79
	L1-L2	R	13821.65	14064.30	242.64	2537.80	0.63
P10	L1-2	R	14286.61	14382.98	96.36	2737.63	0.59
MEAN		**9/7**	**11136.69**	**12184.75**	**1048.06**	**3622.51**	**0.49**
SD			**±3616.94**	**±3453.64**	**±605.68**	**±1573.42**	**±0.17**

Right(R), left (L)

Table 11. Volumetric measurements on the left side

			Left (n=7)				
Patient ID	**Treated segment**	**Side of discoplasty R/L**	**Substracted cylinder volumes (preop mm3)**	**Substracted cylinder volumes (Postop mm3)**	**Delta volume (mm3)**	**PMMA volume (mm3)**	**Distributuion of total PMMA (%)**
P01	L4-5	R	12486.38	13883.91	1397.53	3594.41	0.36
P02	L2-3	R	8898.75	9833.28	934.52	4548.78	0.72
	L3-4	L	11450.70	13075.03	1624.33	3670.57	0.44
	L4-5	L	9841.97	11704.20	1862.23	2986.59	0.47
P03	L5-S1	L	5867.54	7965.47	2097.93	6818.30	0.67

P04	L3-4	L	13057.79	14029.64	971.84	4136.37	0.66
P05	L5-S1	R	7163.45	9453.71	2290.26	4864.38	0.46
P06	L1-2	R	9660.80	10382.86	722.06	3380.00	0.67
P07	L2-3	L	13090.17	13874.83	784.65	1967.92	0.33
	L3-4	L	13794.85	14700.49	905.63	3486.42	0.36
	L4-5	R	11554.23	13513.56	1959.33	4617.84	0.49
P08	L3-4	L	9882.17	10490.94	608.76	6945.22	0.82
	L4-5	R	13308.34	15055.78	1747.43	8336.24	0.71
P09	Th12-L1	R	9933.42	10162.75	229.32	939.35	0.21
	L1-L2	R	8793.31	9027.19	233.88	1495.92	0.37
P10	L1-2	R	9774.92	10071.59	296.66	1911.28	0.41
MEAN		**9/7**	**10534.93**	**11701.58**	**1166.65**	**3981.23**	**0.51**
SD			**±2285.76**	**±2283.32**	**±691.01**	**±2048.44**	**±0.17**

Right (R), left (L)

Table 12. Volumetric comparison of the injection and the contralateral sides

	Side of PMMA injection (Mean±SD)	Contralateral (Mean±SD)	p
Substracted cylinder volumes (preop mm3)	11216.46±2656.45	10455.15±3336.78	0.361
Substracted cylinder volumes (postop mm3)	12318.87±2295.41	11567.45±3419.88	0.468
Delta volume (mm3)	1102.41±646.08	1112.30±659.05	0.724
PMMA volume (mm3)	3912.19±1756.92	3691.54±1904.63	0.985
Distribution of total PMMA	0.52±0.17	0.48±0.17	0.696

4.3. Adjacent segment degeneration after short segment lumbar fusions

A total of hundred patients were eligible for the study. Fifteen subjects were excluded from the final analysis due to incomplete dataset (n=12) or surgical site infection (n=3). Total of 85 subjects were included in the present analysis, of those 62 underwent single- and 23 underwent two-level open transforaminal lumbar interbody fusion (TLIF). Based on our ASD definition (detailed in paragraph, *3.2.1.1.2 Sagittal plane*) 31 of the 85 patients (21 female and 10 male) developed ASD. The incidence of subsequent surgery was 17.6% (15/85)-ranging between 6 months to 4 years (2.69±2.04 years).

4.3.1. Demographics and surgery related factors

Age was significantly higher in ASD group compared to the non-ASD group (47.1±11.6 years vs 54.2±10.4 years, *p=0.007*). ASD patients reported higher pain intensity preoperatively (6.8±2.2 vs 7.8±1.7, *p=0.048*) as well as at follow-up (4.6±2.9 vs. 6.5±2.5, *p=0.004*). Based on ODI increased disability was found in ASD group compared to non-ASD group (27.0±20.3 vs. 38.3±21.8, *p=0.020*) at the endpoint. In regards of surgery related factors, upper-level lumbar fusion was more frequent in ASD group (6% vs 26%, Chi-square=3.99, *p=0.007*) (**Table 13**).

Table 13. Demographic characteristics and surgical details in study cohort

Demographics	**Non-ASD n=54**	**ASD n=31**	**p**
Age, years (mean±SD)	47.1±11.6	54.2±10.4	**0.007**
Gender (M/F)	19/35	10/21	0.784
BMI, kg/m^2(mean±SD)	27.3±5.1	28.5±4.8	0.264
Pain (preop)	6.8±2.2	7.8±1.7	**0.048**
ODI (preop)	44.4±18.1	48.1±14.3	0.326
Pain (FU)	4.6±2.9	6.5±2.5	**0.004**
ODI (FU)	27.0±20.3	38.4±21.8	**0.020**
Surgical details			
Length of Fusion (one/two-level, %)	41/13 (76%/24%)	20/11 (65%/35%)	0.261
Upper/Lower lumbar fusion# (upper/lower, %)	3/51 (6%/94%)	8/23 (26%/74%)	**0.007**
Inclusion of sacrum (yes/no, %)	33/21 (61%/39%)	16/15 (51%/49%)	0.394

Differences between Non-ASD and ASD groups in demographics and surgical details

Adjacent segment degeneration (ASD), body mass index (BMI), Oswestry Disability Index (ODI), Follow-up (FU)

4.3.2. MRI phenotypes, intervertebral disc characteristics

Pfirrmann grade III or higher disc degeneration at the adjacent level before the index surgery was more frequent in the ASD group (24% vs 51%, Chi-square=9.70, *p=0.002*). The presence of disc bulge/herniation was three times higher in ASD patients (11% vs 35%, Chi-square=7.31, *p=0.007*). Major degenerative signs (Pfirrmann grade III or higher disc degeneration and/or presence of disc bulge/protrusion or herniation) were more common in ASD cases (30% vs 64%, Chi-square=9.81, *p=0.002*) (**Table 14**).

Table 14. Distribution of preoperative MRI phenotypes

MRI phenotype	Non-ASD n=54	ASD n=31	p
Disc degeneration	13 (24%)	16 (51%)	**0.002**
Disc bulge/herniation	6 (11%)	11 (35%)	**0.007**
Endplate damage	43 (80%)	26 (84%)	0.630
Annular fissure	1 (2%)	1 (3%)	0.116
Modic change	22 (41%)	18 (58%)	0.124
Major degenerative sign	16 (30%)	20 (64%)	**0.002**

Comparison of ASD and Non-ASD groups (p-values in bold indicate significant difference). Pfirrmann grade III or higher disc degeneration and/or presence of disc bulge/protrusion or herniation were considered as *major degenerative sign. Adjacent segment degeneration (ASD)*

4.3.3. Spinopelvic parameters

Preoperative L4-S1, PI-LL mismatch and PT showed difference between ASD and non-ASD groups. L4-S1 lordosis was significantly lower in ASD group (32.9°±8.8° vs 29.0°±7.3°, *p=0.039*). PI-LL mismatch was greater in ASD patients (-2.3°±9.7° vs 3.2°±11.5°, *p=0.021*). PT was higher in ASD group, which proved a trend to significant difference (14.4°±7.5° vs 17.7°±7.9°, *p=0.056*). **Table 15** represents the difference in radiologic parameters between Non-ASD and ASD groups before the index surgery.

Table 15. Comparison of preoperative spinopelvic parameters

Preop X-ray	**Non-ASD n=54**	**ASD n=31**	**p**
Pelvic Incidence (°)	52.9±11.6	56.9±12.5	0.141
Sacral Slope (°)	38.2±8.9	39.6±9.6	0.493
Pelvic Tilt (°)	14.4±7.5	17.7±7.9	*0.056*
Lumbar Lordosis (°)	55.2±12.4	53.7±13.0	0.601
L4-S1 lordosis (°)	32.9±8.8	29.0±7.3	**0.039**
Segmental Lordosis in Fusion site (°)	12.8±7.2	10.9±6.4	0.215
PI-LL mismatch	-2.3±9.7	3.2±11.5	**0.021**

Adjacent segment degeneration (ASD)

In contrast, postoperative spinopelvic parameters showed no significant differences between groups. **Table 16** represents the difference in radiologic parameters between Non-ASD and ASD groups after the index surgery.

Table 16. Comparison of postoperative spinopelvic parameters

Postop X-ray	**Non-ASD n=54**	**ASD n=31**	**p**
Pelvic Incidence (°)	52.4±11.9	56.7±12.4	0.122
Sacral Slope (°)	35.2±8.9	38.1±8.6	0.163
Pelvic Tilt (°)	17.2±6.9	18.9±7.8	0.309
Lumbar Lordosis (°)	48.2±12.6	51.5±10.9	0.218
L4-S1 lordosis (°)	31.6±9.4	28.3±9.2	0.130
Segmental Lordosis in Fusion site (°)	13.0±6.9	13.7±6.4	0.647
PI-LL mismatch	4.3±9.3	5.2±8.9	0.657

Adjacent segment degeneration (ASD)

4.3.4. Multiparametric model for ASD

Parameters that were not distributed equally across groups were entered into the multivariate logistic regression model: age, upper or lower lumbar fusion, preoperative

L4-S1 lordosis, preoperative PI-LL mismatch and preoperative PT as spinopelvic parameters and the presence of major degenerative sign on preoperative MRI. After application of stepwise backward conditional method, the presence of *major degenerative sign* remained a significant predictor of developing ASD with an OR of 3.85 (CI 95%=1.43-10.37, p= 0.006). (**Table 17**)

Table 17. Multivariate regression model for ASD

Variables	**Result of step 1. of stepwise multivariate regression model for ASD**			
	B (SE)	**Wald**	**OR (95% CI)**	**p**
Age	0.03 (0.03)	0.65	1.025 (0.965-1.089)	0.422
Pelvic Tilt (preoperative)	0.32 (0.05)	0.47	1.032 (0.943-1.130)	0.494
LIV-SI Lordosis (preoperative)	-0.03 (0.03)	0.87	0.966 (0.900-1.038)	0.350
PI-LL mismatch (preoperative)	0.01 (0.03)	0.09	1.011 (0.941-1.086)	0.760
Level of Fusion	1.17 (0.83)	1.98	3.226 (0.633-16.456)	0.159
Major degenerative sign (preoperative)	0.78 (0.64)	1.47	2.183 (0.618-7.703)	0.225
Variables	**Final result of stepwise multivariate regression model for ASD**			
	B (SE)	**Wald**	**OR (95% CI)**	**p**
Major degenerative sign (preoperative)	*1.34 (0.50)*	*7.13*	*3.853 (1.432-10.365)*	***0.006***

Adjacent segment degeneration (ASD)

4.3.5. Subsequent surgeries

In the cases where subsequent surgery was needed, MRI findings before the reoperation in the adjacent segments were the followings: all cases showed advanced disc degeneration, 7 cases developed moderate to severe spinal canal stenosis (7/15, 46.6%), 9 patients showed large disc protrusion (9/15, 60%) and 3 cases developed disc extrusion (3/15, 20%). The Table 18 represents the morphological conditions in details of adjacent segments discussing disc displacements, endplate defects, facet and yellow ligament conditions. (**Table 18**)

No	Level of ASD	Fusion extension	Adjacent Segment pathology on MRI
1	L3-4	Cranial	Severe canal stenosis, central protrusion and yellow ligament hypertrophy
2	L3-4	Cranial	Severe central canal stenosis, central protrusion, disc degeneration, endplate defect
3	L5-S1	Caudal	Severe disc degeneration, advanced Pfirrmann and endplate condition, facet arthrosis
4	L3-4	Cranial	Central canal zone herniation, severe canal stenosis
5	L2-3	Cranial	Central canal stenosis, protrusion
6	L3-4	Cranial	Moderate canal stenosis, subarticular zone herniation
7	L3-4	Cranial	Severe canal stenosis, central canal zone protrusion
8	L4-5	Cranial	Moderate foraminal stenosis, foraminal zone protrusion
9	L2-3	Cranial	Severe disc degeneration, endplate defect, moderate facet arthrosis
10	L2-3	Cranial	Foraminal protrusion and stenosis
11	L3-4, L5-S1	Cranio-caudal	Severe disc degeneration, canal stenosis, facet arthrosis,
12	L4-5	Cranial	Severe canal stenosis, central canal zone disc herniation
13	L2-3, L5-S1	Cranio-caudal	Foraminal zone stenosis, protrusion cranially, subarticular zone protrusion caudally
14	L2-3	Cranial	Moderate lateral recess stenosis, protrusion
15	L4-5	Cranial	Central canal zone protrusion

Table 18. Morphological indications for the subsequent adjacent level surgeries

Adjacent segment degeneration (ASD), L indicates lumbar.

DOI:10.14753/SE.2022.2689

5. Discussion

This dissertation addressed two specific disc degeneration related conditions which have a great impact on clinical management and long-term outcomes.

In the ageing population, advanced stage disc degeneration contributes to poor quality of life and severe disabilities which then may require spinal surgery. In my PhD work the effects of minimally invasive percutaneous cement discoplasty on radiological parameters and clinical outcome were analysed. As a second step, the PCD related indirect foraminal decompression were investigated, applying 3D in silico method and measurements.

Adjacent segment degeneration related pain and disability are one of the main reasons of lumbar revision surgeries worldwide. Factors leading to ASD have been studied extensively, but the aetiology remains unclear. Demographic, surgery related and radiological factors that may influence the development of ASD were analysed.

The results of each study will be discussed in detail in the following chapter.

5.1. Percutaneous cement discoplasty: effect on radiological parameters and clinical outcome

In the clinical study of percutaneous cement discoplasty, the effect of a minimal invasive surgical procedure on lumbar segmental and global radiological parameters and clinical outcome were investigated. Disability and pain significantly improved due to the PCD procedure and the clinical improvement at 6 months follow-up (17.5 points in ODI, 2.4 points in LBP, and 2.9 points in LP) was more than the consensual cut-off values for minimal important change of ODI and pain VAS [100]. Although, pain relief and functional improvement are multidimensional phenomena, this clinical benefit of the PCD procedure on the morphological parameters of the lumbar spine cannot be disputed. The improvement of the patients' disability can be linked to the improvement of the sagittal spinopelvic alignment. We found a positive correlation between the increased sacral slope due to the surgery and the postoperative functional capacity (i.e. decreased ODI). This association was previously demonstrated in adult deformity patients after correction surgery [101–104] and the strength of the correlation what we found was similar to the results of previously published data [101,103]. Pain weakly but

significantly correlated with the changes of some segmental parameters such as the correction of the segmental scoliosis and the disc height. Beyond the segmental stabilization effect of the procedure, both associations can be explained by the change of the foraminal area [105] and the consequent indirect decompression effect [105–107] of PCD which was clearly showed by the radiological parameters.

In the treated segments (i.e. in pain generator vacuum discs), the preoperative anterior disc height significantly reduced compared to the untreated discs (4.5±2.1mm vs. 6.8±2.8mm, $p<0.001$) while the mean posterior disc height was not different in the two subgroups. A decreased IPH (28.8±3.6mm vs. 31.4±4.0mm, $p<0.001$) as well as a decreased segmental lordosis (3.2±3.4° vs. 5.9±3.8°, $p<0.001$) were measured in the severely degenerated discs', candidate for PCD. These results showed the effect of the advanced disc degeneration on the morphology of the motion segment. In this context, the favourable effect of the MIS procedure on these parameters were more straightforward. Due to the PCD, not only, the improvement of the above-mentioned parameters, but also a significant increase in the posterior disc height (DHP) were noticed. The segmental indirect decompression effect of the procedure - characterized by the increased IPH and DHP – was also associated with the correction of the segmental sagittal and coronal alignment. A significant improvement in the global coronal alignment and in segmental lordosis and scoliosis was observed even in the untreated segments. This latter association can be explained by the pain relief and the consequent reduction of the antalgic posture which also relates to the observed improvement of the functional capacity of the patients [108]. Multilevel PCDs had a higher impact on the decrease of lumbar scoliosis.

Our work highlights the positive influence of PCD on global and segmental spinopelvic radiological parameters and their association with clinical outcome. However, the study had some limitations. Dataset of 63 consecutive patients operated between 2014 and 2016 were analysed, but patients having other concomitant open surgeries (n=11, 17.5%), incomplete follow-up data (n=4, 6.3%), having a surgical complication (cement leakage) (n=3, 4.7%) or procedures performed out segments L1-5 (n=17, 26.2%) were excluded from the final study cohort. Although the cohort provided a good power of the study, the excluded subjects could modify the results. The number of the patients with prospective dataset was low, but the analyses of all their L1-5

segments provided a good power of the study. Full standing X-ray was available only for a subset of patients, so influence of PCD on the global alignment is not known. The pain relieving effect of the segmental stabilization (ie. ROM reduction) is alone not known, thus the clinical result of the different dimensions of the procedure (stabilization, indirect decompression, alignment correction) have not been elucidated so far. To validate our results and to clarify the above mentioned biomechanical and clinical issues further biomechanical studies and multicenter clinical trials with long-term follow-up and are needed.

5.2. In silico analysis of discoplasty

Based on the facts about the clinical relevance of PCD mentioned in the previous section, PCD was an applicable option for patients suffering from severe disc degeneration related pain and disability. One of the major findings was that, indirect decompression played a key role in pain relief [105–107,109]. Increased IPH and DHP can be seen in standing X-rays and they were considered as the signs of indirect decompression. The effect was not quantified as exact volumetric change, due the lack of appropriate 3D measurement procedure. In our institution, we developed a method to measure the volumetric change of the neuroforamen and the canal [84]. It was a more feasible and accurate process with reproducible methodology compared to similar papers [110,111]. In this study, we proved that spinal canal volume increased significantly after the procedure. The volume of the injected bone cement positively correlated with the increase of the spinal canal, as well as the total surface of the PMMA. Pain and disability improved after the procedure, which confirmed our previous findings.

During the operative procedure, the side of the insertion of the working channel for discoplasty depends on the surgeons' preference. The main goal is to insert the trocare from a safer side, to reduce the probability of nerve injury. But - as degeneration is often asymmetric- an appropriately positioned needle could influence the segmental parameters.

In a detailed analysis, the volumetric change at the right and the left sides were assessed. Both the right and the left neuroforamen volumes increased significantly after the procedure, however there were no differences in volumes between sides, even if we

took the side of the operation into consideration. The PMMA intake showed a positive correlation with the increase in both neuroforamen of the segment. Albeit the different filling sides, the distribution of the PMMA inside the disc space proved to be statistically equal. Although the fact of the asymmetric nature of degeneration, a carefully applied prone position and the lack of compensatory muscles spasms (due to muscle relaxants administered during general anaesthesia) may have led to a relaxed state of the spine with favourable, more symmetric intervertebral dimensions. Since this state may have been closer to the optimal anatomically symmetric segmental alignment, it resulted in equal distribution of PMMA.

5.3. Adjacent segment degeneration after short segment lumbar fusions

In this study, we assessed the influence of age, surgery related factors, spinopelvic parameters and preoperative MR findings related to adjacent segment degeneration. We found that the presence of major degenerative signs in the adjacent segment before the index surgery increased the risk of developing ASD. The impact of preoperative disc degeneration in adjacent segments was discussed in previous studies [63,80,112]. In agreement with our findings, some authors also reported that Pfirrmann grade III or higher disc degeneration and presence of disc bulge/protrusion in adjacent segment increased the risk of developing ASD [63,110,113]. Altered biomechanics in adjacent segments may have more profound effect on discs with higher grade degeneration and predispose patients to clinically significant ASD. In line with this observation, every patient who underwent subsequent surgery presented with severe degenerative changes and disc displacements on MRI had significantly higher pain and disability on PROM scores.

Aging of the spine is slow natural process marked by consecutive stages of disc degeneration [30]. In our study, age was not an independent predictor of developing ASD, possibly due to the relative short follow up period.

The current literature is controversial about the impact of instrumentation length and level of fusion as a risk factor leading to ASD [74,79,114]. Patients with upper-level lumbar fusions more frequently developed ASD. The reason might be the difference in range of motions (ROM) in lumbar segments. As Cook et al. described, the ROM of L1-L3 segments were less flexible and more rigid compared to lower segments [45]. In

upper lumbar fusions rigidity limited segmental compensatory mechanisms in adjacent segments and can lead to disc degeneration. Higher pelvic tilt entailed compensatory mechanisms like pelvic retroversion to maintain balance. Although higher PT can lead to increased pain and disability, PT was not proved to be a risk factor of ASD in the final model [36]. Current literature supports this finding [74].

The lumbar lordosis and its distribution are one of the main components in lumbar spine stabilization surgeries. Optimal distribution of L4-S1 lordosis was previously discussed by Yilgor at al. [115]. However, it has never been studied before in the development of ASD. Improper distribution of lordosis had a significant consequence on sagittal alignment and can influence the local biomechanics too [115]. Preoperative L4-S1 lordosis was significantly lower in ASD group, but it was not a predictor of developing ASD in our multivariate regression model.

In this current study LL and PI were not different between groups, however, only ASD patients showed moderate PI-LL mismatch preoperatively according to original classification by Schwab et al [83]. The moderate mismatch combined with mild increase in PT could be the reason of higher preoperative pain in ASD patients [116].

Our study has some limitations, that should be taken into consideration. First, the relatively low number of participants could limit our analysis. We could not analyse radiological and clinical ASD separately due the low number of patients in subgroups. Second, only lumbar spine X-rays were carried out due to technical reasons, so we were not able to calculate global sagittal balance.

However, one important strength of our study is the detailed multidimensional measurements of spinopelvic parameters and spinal motion segments; especially, the multi-aspect MRI analysis, such as the role of endplate defects, annular fissures and Modic changes. Another advantage of the study was the homogenous patient group and the collection of detailed follow-up data as well as the low drop-out rate.

DOI:10.14753/SE.2022.2689

6. Conclusion

As a conclusion, answers will be provided to the research questions each-by-each as listed in objectives.

6.1. Relationship between the change of segmental and regional biomechanics and the clinical effects after percutaneous cement discoplasty

1. *Does PCD lead to significant pain relief and increase in functional capacity?*
   After the procedure, a significant increase was observed in functional capacity in ODI (37.9% decrease) while leg pain (42% decrease) and low back pain (40.6% decrease) significantly decreased.
2. *Does this technique have an impact on the radiologic characteristics for the motion segment?*
   Parameters that describe the intervertebral disc and the neuroforamen showed a significant change as an effect of PCD. Anterior and posterior disc height significantly increased, as well as interpedicular height. There was a significant correction in segmental alignment of the spinal unit.
3. *Does PCD influence the lumbar alignment?*
   Segmental lordosis increased while the segmental scoliosis decreased significantly after the procedure. A mild correction of lumbar scoliosis could be achieved, with a more prominent effect in multilevel PCD.
4. *Is any of the spinopelvic radiologic parameters associated with the clinical outcome?*
   Medium positive association was found between the increase of sacral slope and improvement of ODI postoperatively. The correction of segmental scoliosis was correlated with the reduction of LBP. The increase in DHA correlated with ODI and LP as well, while the changes in DHP were associated with the reduction of LP.

Elderly patients with several comorbities and also suffering from severe disc degeneration are often not suitable for extended open surgeries because of the increased perioperative risk for complications. The main purpose of the minimal invasive PCD

surgery is pain relief and restoration of quality of life. Our results showed that PCD had not only a segmental stabilizing effect but also provided a foraminal decompression and lumbar alignment correction effect, leading to increase in quality of life and reduction in low back and leg pain.

6.2. In silico analysis of indirect decompression after PCD

1. *How does the injected PMMA influence the neuroforaminal dimensions comparing at each side of the segment?*

   As the effect of PCD, the neuroforaminal dimensions showed a significant increase after the procedure in both right and left sides. There was no significant difference in the volume increase between the two sides.

2. *Does the operative technique, especially the side of the PMMA injection influence the volumetric change in the foramen and the PMMA distribution?*

   The side of the workflow introduction did not influence the volumetric increase of the neuroforamen. The distribution of the PMMA inside the disc proved to be equal between both sides.

Our in-silico measurements provided quantitative information of the effect of PCD. Proving our previous clinical findings, that the application of PMMA in intervertebral discs significantly increased the volume of the foramen in both sides. The PCD procedure provided equal distribution of the PMMA inside the disc either filled from left or right side. The injected total volume was strongly associated with the achieved result.

6.3. Incidence and risk factors of adjacent segment degeneration after short segment lumbar fusions

1. *What is the incidence of ASD and what is the rate of ASD related subsequent surgery after routine, short-segment lumbar fusions?*

   According the applied ASD definition, 36.4% (31 of the 85 patients) of the population developed ASD after short segment TLIF, which supported the

scientific literature data. The incidence of subsequent surgery was 17.6% (15 of 85 patients).

2. *Which radiological parameters differ pre- and postoperatively between ASD and non-ASD patients?*

ASD patients showed significantly lower L4-S1 lordosis and increased PI-LL mismatch preoperatively. Pelvic tilt was increased in ASD group with a trend to significant difference. There were no significant differences between groups in radiological parameters in early postoperative x-ray.

3. *Do preoperative or postoperative spinopelvic parameters influence long-term outcome in connection with ASD after short segment lumbar surgeries?*

Although L4-S1 lordosis, PT and PI-LL mismatch were significantly different in ASD group preoperatively, none of them proved to be a significant risk factor of ASD in regression model.

4. *Which preoperative MRI finding can have significant long-term effect on the development of ASD?*

Ongoing preoperative disc degeneration equal or higher than Pfirrmann grade 3 and/or the presence of disc bulge/protrusion (major degenerative signs) significantly increased the likelihood of developing ASD.

5. *What are the main characteristics of the adjacent altered discs that required subsequent surgeries?*

MRI images of the 15 subsequent surgeries showed advanced disc degeneration in all cases, 7 cases developed moderate to severe spinal canal stenosis (7/15, 46.6%), 9 patients showed large disc protrusion (9/15, 60%) and 3 cases developed disc extrusion (3/15, 20%).

Despite the multitude of studies published, the causes of ASD are not understood completely. The role of spinopelvic parameters and other factors that influence, induce or trigger changes in the adjacent mobile segments are still not clear. We found that preoperative major degenerative sign was an independent predictor of developing adjacent segment degeneration. Consequently, adjacent disc conditions should be carefully analysed during surgical planning. If major degenerative signs are present, the inclusion of the segment into the index fusion is considerable.

DOI:10.14753/SE.2022.2689

7. Summary

Low back pain is a common health problem, responsible for the highest disability adjusted life years worldwide, it affects every age group from children to elderly. Yearly, almost 4% of the total population suffer from degenerative spinal disease and associated low back pain. The more information we gather about disc degeneration and related symptoms, the more improvement we reach in spinal care.

Our aim was to analyse specific intervertebral disc conditions that have a great impact in clinical management and long-term outcomes.

Advanced stage disc degeneration is often a polysegmental condition and contributes to poor quality of life, and severe disabilities that may require spinal surgeries. It often occurs with severe comorbities which contraindicate extended open surgeries. To address these clinical conditions minimally invasive percutaneous cement discoplasty was introduced as a salvage technique. We proved that PCD was an effective technique to treat axial pain and disability related to severe lumbar disc degeneration. Our study showed that an improvement in lumbar alignment and a significant indirect foraminal decompression could be achieved with the procedure. These changes can significantly contribute to the pain relief and increase in the patients' functional capacity. The indirect foraminal decompression was verified with a quantitative in silico methodology. According to our findings, volumetric increase in neuroforamen is strongly associated with the injected PMMA volume in both sides. The distribution of PMMA was equal inside the disc space, regardless the side of the operation.

Short lumbar fusions are the most commonly applied surgeries, with possible long-term impact on adjacent discs biomechanics that may contribute pain, disabilities and may lead to revision surgeries. Factors leading to ASD have been studied extensively, but the aetiology remains unclear. In our study, we found that the preoperative presence of major degenerative signs in the adjacent segment before the index surgery increased the risk for developing ASD.

DOI:10.14753/SE.2022.2689

8. Összefoglalás

A derékfájdalom jelentős egészségügyi probléma, mely világszerte a legtöbb rokkantságban, mozgáskorlátozottságban eltöltött életévért felelős. A teljes populáció mintegy 4% szenved degeneratív porckorong betegségtől és következményes derékfájdalomtól. Ennek tekintetében minél több információ áll rendelkezésre a porckorong kopásról és az ahhoz kapcsolódó tünetekről annál hatékonyabbá tehető mindezek gerincgyógyászati ellátása.

Célunk azon speciális porckorong állapotok vizsgálata volt, melyek nagyban befolyásolják a mindennapi betegellátást, valamint a hosszú távú terápiás kimenetelt.

Az előrehaladott porckorong degeneráció általában poliszegmetális állapot, alacsony életminőséghez és mozgáskorlátozottsághoz vezet. Ezen esetekben sokszor műtéti terápia indokolt, azonban a betegcsoportban megjelenő számos, súlyos társbetegség okán kiterjesztett, nyitott gerincműtét sokszor nem végezhető. „Salvage" megoldásként minimal invazív perkután cement diszkoplasztika (PCD) alkalmazható bizonyos esetekben. Vizsgálataink során bebizonyítottuk, hogy a PCD effektív megoldás előrehaladott ágyéki porkorong kopás okozta axiális terhelési derékfájdalom és az ehhez kapcsolódó mozgáskorlátozottság kezelésre. Segítségével a lumbális görbület harmonikusabbá tehető, továbbá szignifikáns indirekt foraminális dekompresszió érhető el. Mindezek a fájdalom csökkenést, valamint a beteg terhelhetőségének és funkcionális kapacitásának növekedését eredményezik. Megfigyeléseinket in silico mérésekkel egészítettük ki, melyek során számszerűen alátámasztottuk, hogy a neuroforamen térfogatnövekedése erős korrelációt mutat a beinjektált PMMA csontcement mennyiségével. Továbbá igazoltuk, hogy PMMA porckorongon belüli eloszlása egyenletes, független a műtét oldaliságától.

Az egy- és két szintes ágyéki fúziók a leggyakrabban elvégzett gerincsebészeti műtéti megoldások közé tartoznak. Ezek a beavatkozások hatást gyakorolnak a szomszédos porckorongok biomechanikájára és hosszú távon fájdalmat és mozgáskorlátozottságot eredményezhetnek, felvetve további gerincműtét szükségességét. Vizsgálatunk során számos demográfiai, sebészi, spinopelvicus és MR eltérést analizálva igazoltuk, hogy a szomszédos szegmentumok preoperatív degenerációja növeli a szomszédos szegmentum szindróma kialakulásának valószínűségét.

9. References

1. Vos T, Flaxman AD, Naghavi M, Lozano R, Michaud C, Ezzati M, Shibuya K, Salomon JA, Abdalla S, Aboyans V, Abraham J, Ackerman I, Aggarwal R, Ahn SY, Ali MK, AlMazroa MA, Alvarado M, Anderson HR, Anderson LM, Andrews KG, Atkinson C, Baddour LM, Bahalim AN, Barker-Collo S, Barrero LH, Bartels DH, Basáñez MG, Baxter A, Bell ML, Benjamin EJ, Bennett D, Bernabé E, Bhalla K, Bhandari B, Bikbov B, Abdulhak AB, Birbeck G, Black JA, Blencowe H, Blore JD, Blyth F, Bolliger I, Bonaventure A, Boufous S, Bourne R, Boussinesq M, Braithwaite T, Brayne C, Bridgett L, Brooker S, Brooks P, Brugha TS, Bryan-Hancock C, Bucello C, Buchbinder R, Buckle G, Budke CM, Burch M, Burney P, Burstein R, Calabria B, Campbell B, Canter CE, Carabin H, Carapetis J, Carmona L, Cella C, Charlson F, Chen H, Cheng ATA, Chou D, Chugh SS, Coffeng LE, Colan SD, Colquhoun S, Colson KE, Condon J, Connor MD, Cooper LT, Corriere M, Cortinovis M, de Vaccaro KC, Couser W, Cowie BC, Criqui MH, Cross M, Dabhadkar KC, Dahiya M, Dahodwala N, Damsere-Derry J, Danaei G, Davis A, De Leo D, Degenhardt L, Dellavalle R, Delossantos A, Denenberg J, Derrett S, Des Jarlais DC, Dharmaratne SD, Dherani M, Diaz-Torne C, Dolk H, Dorsey ER, Driscoll T, Duber H, Ebel B, Edmond K, Elbaz A, Ali SE, Erskine H, Erwin PJ, Espindola P, Ewoigbokhan SE, Farzadfar F, Feigin V, Felson DT, Ferrari A, Ferri CP, Fèvre EM, Finucane MM, Flaxman S, Flood L, Foreman K, Forouzanfar MH, Fowkes FGR, Franklin R, Fransen M, Freeman MK, Gabbe BJ, Gabriel SE, Gakidou E, Ganatra HA, Garcia B, Gaspari F, Gillum RF, Gmel G, Gosselin R, Grainger R, Groeger J, Guillemin F, Gunnell D, Gupta R, Haagsma J, Hagan H, Halasa YA, Hall W, Haring D, Haro JM, Harrison JE, Havmoeller R, Hay RJ, Higashi H, Hill C, Hoen B, Hoffman H, Hotez PJ, Hoy D, Huang JJ, Ibeanusi SE, Jacobsen KH, James SL, Jarvis D, Jasrasaria R, Jayaraman S, Johns N, Jonas JB, Karthikeyan G, Kassebaum N, Kawakami N, Keren A, Khoo JP, King CH, Knowlton LM, Kobusingye O, Koranteng A, Krishnamurthi R, Lalloo R, Laslett LL, Lathlean T, Leasher JL, Lee YY, Leigh J, Lim SS, Limb E, Lin JK, Lipnick M, Lipshultz SE, Liu W, Loane M, Ohno SL, Lyons R, Ma J, Mabweijano J, MacIntyre MF, Malekzadeh R, Mallinger L, Manivannan S, Marcenes W, March L, Margolis DJ,

Marks GB, Marks R, Matsumori A, Matzopoulos R, Mayosi BM, McAnulty JH, McDermott MM, McGill N, McGrath J, Medina-Mora ME, Meltzer M, Memish ZA, Mensah GA, Merriman TR, Meyer AC, Miglioli V, Miller M, Miller TR, Mitchell PB, Mocumbi AO, Moffitt TE, Mokdad AA, Monasta L, Montico M, Moradi-Lakeh M, Moran A, Morawska L, Mori R, Murdoch ME, Mwaniki MK, Naidoo K, Nair MN, Naldi L, Narayan KV, Nelson PK, Nelson RG, Nevitt MC, Newton CR, Nolte S, Norman P, Norman R, O'Donnell M, O'Hanlon S, Olives C, Omer SB, Ortblad K, Osborne R, Ozgediz D, Page A, Pahari B, Pandian JD, Rivero AP, Patten SB, Pearce N, Padilla RP, Perez-Ruiz F, Perico N, Pesudovs K, Phillips D, Phillips MR, Pierce K, Pion S, Polanczyk GV, Polinder S, Pope CA, Popova S, Porrini E, Pourmalek F, Prince M, Pullan RL, Ramaiah KD, Ranganathan D, Razavi H, Regan M, Rehm JT, Rein DB, Remuzzi G, Richardson K, Rivara FP, Roberts T, Robinson C, De Leòn FR, Ronfani L, Room R, Rosenfeld LC, Rushton L, Sacco RL, Saha S, Sampson U, Sanchez-Riera L, Sanman E, Schwebel DC, Scott JG, Segui-Gomez M, Shahraz S, Shepard DS, Shin H, Shivakoti R, Silberberg D, Singh D, Singh GM, Singh JA, Singleton J, Sleet DA, Sliwa K, Smith E, Smith JL, Stapelberg NJ, Steer A, Steiner T, Stolk WA, Stovner LJ, Sudfeld C, Syed S, Tamburlini G, Tavakkoli M, Taylor HR, Taylor JA, Taylor WJ, Thomas B, Thomson WM, Thurston GD, Tleyjeh IM, Tonelli M, Towbin JA, Truelsen T, Tsilimbaris MK, Ubeda C, Undurraga EA, van der Werf MJ, van Os J, Vavilala MS, Venketasubramanian N, Wang M, Wang W, Watt K, Weatherall DJ, Weinstock MA, Weintraub R, Weisskopf MG, Weissman MM, White RA, Whiteford H, Wiersma ST, Wilkinson JD, Williams HC, Williams SR, Witt E, Wolfe F, Woolf AD, Wulf S, Yeh PH, Zaidi AK, Zheng ZJ, Zonies D, Lopez AD, Murray CJ. Years lived with disability (YLDs) for 1160 sequelae of 289 diseases and injuries 1990–2010: a systematic analysis for the Global Burden of Disease Study 2010. The Lancet. 2012 Dec;380(9859):2163–2196.

2. Ravindra VM, Senglaub SS, Rattani A, Dewan MC, Härtl R, Bisson E, Park KB, Shrime MG. Degenerative Lumbar Spine Disease: Estimating Global Incidence and Worldwide Volume. Global Spine Journal. 2018 Dec;8(8):784–794.

3. Raj PP. Intervertebral Disc: Anatomy-Physiology-Pathophysiology-Treatment. Pain Practice. 2008 Jan;8(1):18–44.

4. Baaj AA, Mummaneni PV, Uribe JS, Vaccaro AR, Greenberg MS, editors. Handbook of spine surgery. Second edition. New York Stuttgart Delhi Rio de Janeiro: Thieme; 2016. 533 p.

5. Tomaszewski KA, Saganiak K, Gładysz T, Walocha JA. The biology behind the human intervertebral disc and its endplates. Folia Morphol. 2015;74(2):12.

6. Colombier P, Clouet J, Hamel O, Lescaudron L, Guicheux J. The lumbar intervertebral disc: From embryonic development to degeneration. Joint Bone Spine. 2014 Mar;81(2):125–129.

7. Kapandji IA. The physiology of the joints. 6th ed., English ed. Edinburgh ; New York: Churchill Livingstone; 2007. 1 p.

8. Chan SCW, Ferguson SJ, Gantenbein-Ritter B. The effects of dynamic loading on the intervertebral disc. Eur Spine J. 2011 Nov;20(11):1796–1812.

9. Neidlinger-Wilke C, Galbusera F, Pratsinis H, Mavrogonatou E, Mietsch A, Kletsas D, Wilke HJ. Mechanical loading of the intervertebral disc: from the macroscopic to the cellular level. Eur Spine J. 2014 Jun;23(S3):333–343.

10. Oxland TR. Fundamental biomechanics of the spine—What we have learned in the past 25 years and future directions. Journal of Biomechanics. 2016 Apr;49(6):817–832.

11. Wilke HJ, Neef P, Hinz B, Seidel H, Claes L. Intradiscal pressure together with anthropometric data – a data set for the validation of models. Clinical Biomechanics. 2001 Jan;16:S111–126.

12. Donohue PJ, Jahnke MR, Blaha JD, Caterson B. Characterization of link protein(s) from human intervertebral-disc tissues. Biochemical Journal. 1988 May 1;251(3):739–747.

13. Feng H, Danfelter M, Strömqvist B, Heinegård D. Extracellular Matrix in Disc Degeneration. VO LU M E. :5.

14. Vernon-Roberts B, Moore RJ, Fraser RD. The Natural History of Age-related Disc Degeneration. :8.

15. Adams MA, Roughley PJ. What is Intervertebral Disc Degeneration, and What Causes It?: Spine. 2006 Aug;31(18):2151–2161.

16. Roberts S, Evans H, Trivedi J, Menage J. Histology and Pathology of the Human Intervertebral Disc. VO LU M E. :5.

17. Adams MA, Roughley PJ. What is Intervertebral Disc Degeneration, and What Causes It?: Spine. 2006 Aug;31(18):2151–2161.

18. Moore R, Fraser RD, Osti L, Vernon-Roberts B. 0. L. OSTI, B. VERNON-ROBERTS,. THE JOURNAL OF BONE AND JOINT SURGERY. 1992;74(5):5.

19. Pfirrmann CWA, Metzdorf A, Zanetti M, Hodler J, Boos N. Magnetic Resonance Classification of Lumbar Intervertebral Disc Degeneration: Spine. 2001 Sep;26(17):1873–1878.

20. Modic MT, Masaryk TJ, Ross JS, Carter JR. Imaging of degenerative disk disease. Radiology. 1988 Jul;168(1):177–186.

21. D'Anastasi M, Birkenmaier C, Schmidt GP, Wegener B, Reiser MF, Baur-Melnyk A. Correlation Between Vacuum Phenomenon on CT and Fluid on MRI in Degenerative Disks. American Journal of Roentgenology. 2011 Nov;197(5):1182–1189.

22. Iguchi T, Ozaki T, Chin T, Tsumura N, Kanemura A, Kasahara K, Kuroda R, Doita M, Nishida K. Intimate relationship between instability and degenerative signs at L4/5 segment examined by flexion–extension radiography. Eur Spine J. 2011 Aug;20(8):1349–1354.

23. Leone A, Guglielmi G, Cassar-Pullicino VN, Bonomo L. Lumbar Intervertebral Instability: A Review. Radiology. 2007 Oct;245(1):62–77.

24. Rajasekaran S, Venkatadass K, Naresh Babu J, Ganesh K, Shetty AP. Pharmacological enhancement of disc diffusion and differentiation of healthy, ageing and degenerated discs: Results from in-vivo serial post-contrast MRI studies in 365 human lumbar discs. Eur Spine J. 2008 May;17(5):626–643.

25. Natarajan RN, Ke JH, Andersson GBJ. A Model to Study the Disc Degeneration Process: Spine. 1994 Feb;19(3):259–264.

26. Adams MA, Dolan P. Intervertebral disc degeneration: evidence for two distinct phenotypes. J Anat. 2012 Dec;221(6):497–506.

27. Rajasekaran S, Babu JN, Arun R, Armstrong BRW, Shetty AP, Murugan S. ISSLS Prize Winner: A Study of Diffusion in Human Lumbar Discs: A Serial Magnetic Resonance Imaging Study Documenting the Influence of the Endplate on Diffusion in Normal and Degenerate Discs: Spine. 2004 Dec;29(23):2654–2667.

28. Rajasekaran S, Venkatadass K, Naresh Babu J, Ganesh K, Shetty AP. Pharmacological enhancement of disc diffusion and differentiation of healthy, ageing and degenerated discs: Results from in-vivo serial post-contrast MRI studies in 365 human lumbar discs. Eur Spine J. 2008 May;17(5):626–643.

29. Zhang YH, Zhao CQ, Jiang LS, Chen XD, Dai LY. Modic changes: a systematic review of the literature. Eur Spine J. 2008 Oct;17(10):1289–1299.

30. Kushchayev SV, Glushko T, Jarraya M, Schuleri KH, Preul MC, Brooks ML, Teytelboym OM. ABCs of the degenerative spine. Insights Imaging. 2018 Apr;9(2):253–274.

31. Izzo R, Popolizio T, D'Aprile P, Muto M. Spinal pain. European Journal of Radiology. 2015 May;84(5):746–756.

32. Jinkins JR. Acquired degenerative changes of the intervertebral segments at and suprajacent to the lumbosacral junction. European Journal of Radiology. 2004 May;50(2):134–158.

33. Fujiwara A, Lim TH, An HS, Tanaka N, Jeon CH, Andersson GBJ, Haughton VM. The Effect of Disc Degeneration and Facet Joint Osteoarthritis on the Segmental Flexibility of the Lumbar Spine: Spine. 2000 Dec;25(23):3036–3044.

34. Legaye J, Duval-Beaup�re G, Marty C, Hecquet J. Pelvic incidence: a fundamental pelvic parameter for three-dimensional regulation of spinal sagittal curves. European Spine Journal. 1998 May 5;7(2):99–103.

35. Duval-Beaupère G, Schmidt C, Cosson P. A barycentremetric study of the sagittal shape of spine and pelvis: The conditions required for an economic standing position. Ann Biomed Eng. 1992 Jul;20(4):451–462.

36. Le Huec JC, Thompson W, Mohsinaly Y, Barrey C, Faundez A. Sagittal balance of the spine. Eur Spine J. 2019 Sep;28(9):1889–1905.

37. Yilgor C, Sogunmez N, Boissiere L, Yavuz Y, Obeid I, Kleinstück F, Pérez-Grueso FJS, Acaroglu E, Haddad S, Mannion AF, Pellise F, Alanay A. Global Alignment and Proportion (GAP) Score: Development and Validation of a New Method of Analyzing Spinopelvic Alignment to Predict Mechanical Complications After Adult Spinal Deformity Surgery. The Journal of Bone and Joint Surgery. 2017 Oct 4;99(19):1661–1672.

38. Schwab F, Ungar B, Blondel B, Buchowski J, Coe J, Deinlein D, DeWald C, Mehdian H, Shaffrey C, Tribus C, Lafage V. Scoliosis Research Society—Schwab Adult Spinal Deformity Classification: A Validation Study. Spine. 2012 May;37(12):1077–1082.

39. Roussouly P, Nnadi C. Sagittal plane deformity: an overview of interpretation and management. Eur Spine J. 2010 Nov;19(11):1824–1836.

40. Le Huec JC, Hasegawa K. Normative values for the spine shape parameters using 3D standing analysis from a database of 268 asymptomatic Caucasian and Japanese subjects. Eur Spine J. 2016 Nov;25(11):3630–3637.

41. Le Huec JC, Demezon H, Aunoble S. Sagittal parameters of global cervical balance using EOS imaging: normative values from a prospective cohort of asymptomatic volunteers. Eur Spine J. 2015 Jan;24(1):63–71.

42. Balagué F, Mannion AF, Pellisé F, Cedraschi C. Non-specific low back pain. The Lancet. 2012 Feb;379(9814):482–491.

43. Le Huec JC, Thompson W, Mohsinaly Y, Barrey C, Faundez A. Sagittal balance of the spine. Eur Spine J. 2019 Sep;28(9):1889–1905.

44. Jackson RP, McManus AC. Radiographic Analysis of Sagittal Plane Alignment and Balance in Standing Volunteers and Patients with Low Back Pain Matched for Age, Sex, and Size: A Prospective Controlled Clinical Study. Spine. 1994 Jul;19(Supplement):1611–1618.

45. Cook DJ, Yeager MS, Cheng BC. Range of Motion of the Intact Lumbar Segment: A Multivariate Study of 42 Lumbar Spines. Int J Spine Surg. 2015;9:5.

46. Sola C, Camino Willhuber G, Kido G, Pereira Duarte M, Bendersky M, Mereles M, Petracchi M, Gruenberg M. Percutaneous cement discoplasty for the treatment of advanced degenerative disk disease in elderly patients. Eur Spine J. 2021 Aug;30(8):2200–2208.

47. Varga PP, Jakab G, Bors IB, Lazary A, Szövérfi Z. Experiences with PMMA cement as a stand-alone intervertebral spacer: Percutaneous cement discoplasty in the case of vacuum phenomenon within lumbar intervertebral discs. English Version. Orthopäde. 2015 Nov;44(S1):1–8.

48. Hou Y, Luo Z. A Study on the Structural Properties of the Lumbar Endplate: Histological Structure, the Effect of Bone Density, and Spinal Level. Spine. 2009 May;34(12):E427–433.

49. Uddin OM, Haque R, Sugrue PA, Ahmed YM, El Ahmadieh TY, Press JM, Koski T, Fessler RG. Cost minimization in treatment of adult degenerative scoliosis. SPI. 2015 Dec;23(6):798–806.

50. Lewandrowski KU, Schubert MD, Ramirez Leon JF, Fessler RG. Minimally invasive spinal surgery: principles and evidence-based practice. 2018.

51. Tye EY, Alentado VJ, Mroz TE, Orr RD, Steinmetz MP. Comparison of Clinical and Radiographic Outcomes in Patients Receiving Single-Level Transforaminal Lumbar Interbody Fusion With Removal of Unilateral or Bilateral Facet Joints. Spine. 2016 Sep;41(17):E1039–1045.

52. Phillips FM, Slosar PJ, Youssef JA, Andersson G, Papatheofanis F. Lumbar Spine Fusion for Chronic Low Back Pain Due to Degenerative Disc Disease: A Systematic Review. Spine. 2013 Apr;38(7):E409–422.

53. Lee CK, Langrana NA. Lumbosacral Spinal Fusion A Biomechanical Study: Spine. 1984 Sep;9(6):574–581.

54. Ekman P, Möller H, Shalabi A, Yu YX, Hedlund R. A prospective randomised study on the long-term effect of lumbar fusion on adjacent disc degeneration. Eur Spine J. 2009 Aug;18(8):1175–1186.

55. Moreau PE, Ferrero E, Riouallon G, Lenoir T, Guigui P. Radiologic adjacent segment degeneration 2 years after lumbar fusion for degenerative spondylolisthesis. Orthopaedics & Traumatology: Surgery & Research. 2016 Oct;102(6):759–763.

56. Imagama S, Kawakami N, Matsubara Y, Tsuji T, Ohara T, Katayama Y, Ishiguro N, Kanemura T. Radiographic Adjacent Segment Degeneration at 5 Years After L4/5 Posterior Lumbar Interbody Fusion With Pedicle Screw Instrumentation: Evaluation by Computed Tomography and Annual Screening With Magnetic Resonance Imaging. Clinical Spine Surgery: A Spine Publication. 2016 Nov;29(9):E442–451.

57. Nakashima H, Kawakami N, Tsuji T, Ohara T, Suzuki Y, Saito T, Nohara A, Tauchi R, Ohta K, Hamajima N, Imagama S. Adjacent Segment Disease After Posterior Lumbar Interbody Fusion: Based on Cases With a Minimum of 10 Years of Follow-up. Spine. 2015 Jul;40(14):E831–841.

58. Zhang C, Berven SH, Weber MH. Adjacent Segment Degeneration Versus Disease After Lumbar Spine Fusion for Degenerative Pathology. 2016;29(1):9.

59. Trivedi NN, Wilson SM, Puchi LA, Lebl DR. Evidence-Based Analysis of Adjacent Segment Degeneration and Disease After LIF: A Narrative Review. Global Spine Journal. 2018 Feb;8(1):95–102.

60. Xia XP, Chen HL, Cheng HB. Prevalence of Adjacent Segment Degeneration After Spine Surgery: A Systematic Review and Meta-analysis. Spine. 2013 Apr;38(7):597–608.

61. Cheh G, Bridwell KH, Lenke LG, Buchowski JM, Daubs MD, Kim Y, Baldus C. Adjacent Segment Disease FollowingLumbar/Thoracolumbar Fusion With Pedicle Screw Instrumentation: A Minimum 5-Year Follow-up. Spine. 2007 Sep;32(20):2253–2257.

62. Okuda S, Nagamoto Y, Matsumoto T, Sugiura T, Takahashi Y, Iwasaki M. Adjacent Segment Disease After Single Segment Posterior Lumbar Interbody Fusion for Degenerative Spondylolisthesis: Minimum 10 Years Follow-up. Spine. 2018 Dec 1;43(23):E1384–1388.

63. Kim KH, Lee SH, Shim CS, Lee DY, Park HS, Pan WJ, Lee HY. Adjacent Segment Disease After Interbody Fusion and Pedicle Screw Fixations for Isolated L4–L5 Spondylolisthesis: A Minimum Five-Year Follow-up. Spine. 2010 Mar;35(6):625–634.

64. Yang JY, Lee JK, Song HS. The Impact of Adjacent Segment Degeneration on the Clinical Outcome After Lumbar Spinal Fusion: Spine. 2008 Mar;33(5):503–507.

65. Kanayama M, Togawa D, Hashimoto T, Shigenobu K, Oha F. Motion-preserving Surgery Can Prevent Early Breakdown of Adjacent Segments: Comparison of Posterior Dynamic Stabilization With Spinal Fusion. Journal of Spinal Disorders & Techniques. 2009 Oct;22(7):463–467.

66. Ghiselli G, Wang JC, Bhatia NN, Hsu WK, Dawson EG. ADJACENT SEGMENT DEGENERATION IN THE LUMBAR SPINE: The Journal of Bone and Joint Surgery-American Volume. 2004 Jul;86(7):1497–1503.

67. Park P, Garton HJ, Gala VC, Hoff JT, McGillicuddy JE. Adjacent Segment Disease after Lumbar or Lumbosacral Fusion: Review of the Literature: Spine. 2004 Sep;29(17):1938–1944.

68. Heo Y, Park JH, Seong HY, Lee YS, Jeon SR, Rhim SC, Roh SW. Symptomatic adjacent segment degeneration at the L3–4 level after fusion surgery at the L4–5 level: evaluation of the risk factors and 10-year incidence. Eur Spine J. 2015 Nov;24(11):2474–2480.

69. Chen CS, Cheng CK, Liu CL, Lo WH. Stress analysis of the disc adjacent to interbody fusion in lumbar spine. Medical Engineering & Physics. 2001 Sep;23(7):485–493.

70. Lee JC, Kim Y, Soh JW, Shin BJ. Risk Factors of Adjacent Segment Disease Requiring Surgery After Lumbar Spinal Fusion: Comparison of Posterior Lumbar Interbody Fusion and Posterolateral Fusion. Spine. 2014 Mar;39(5):E339–345.

71. Irmola TM, Häkkinen A, Järvenpää S, Marttinen I, Vihtonen K, Neva M. Reoperation Rates Following Instrumented Lumbar Spine Fusion. Spine. 2018 Feb 15;43(4):295–301.

72. Lau KKL, Samartzis D, To NSC, Harada GK, An HS, Wong AYL. Demographic, Surgical, and Radiographic Risk Factors for Symptomatic Adjacent Segment Disease After Lumbar Fusion: A Systematic Review and Meta-Analysis. Journal of Bone and Joint Surgery. 2021 Aug 4;103(15):1438–1450.

73. Phan K, Nazareth A, Hussain AK, Dmytriw AA, Nambiar M, Nguyen D, Kerferd J, Phan S, Sutterlin C, Cho SK, Mobbs RJ. Relationship between sagittal balance and adjacent segment disease in surgical treatment of degenerative lumbar spine disease: meta-analysis and implications for choice of fusion technique. Eur Spine J. 2018 Aug;27(8):1981–1991.

74. Wang T, Ding W. Risk factors for adjacent segment degeneration after posterior lumbar fusion surgery in treatment for degenerative lumbar disorders: a meta-analysis. J Orthop Surg Res. 2020 Dec;15(1):582.

75. Bagheri SR, Alimohammadi E, Zamani Froushani A, Abdi A. Adjacent segment disease after posterior lumbar instrumentation surgery for degenerative disease: Incidence and risk factors. J Orthop Surg (Hong Kong). 2019 May;27(2):230949901984237.

76. Gillet P. The Fate of the Adjacent Motion Segments After Lumbar Fusion. J Spinal Disord. 2003;16(4):8.

77. Roussouly P, Pinheiro-Franco JL. Biomechanical analysis of the spino-pelvic organization and adaptation in pathology. Eur Spine J. 2011 Sep;20(S5):609–18.

78. Wang H, Ma L, Yang D, Wang T, Liu S, Yang S, Ding W. Incidence and risk factors of adjacent segment disease following posterior decompression and instrumented fusion for degenerative lumbar disorders. Medicine. 2017 Feb;96(5):e6032.

79. Anandjiwala J, Seo JY, Ha KY, Oh IS, Shin DC. Adjacent segment degeneration after instrumented posterolateral lumbar fusion: a prospective cohort study with a minimum five-year follow-up. Eur Spine J. 2011 Nov;20(11):1951–1960.

80. Liang J, Dong Y, Zhao H. Risk factors for predicting symptomatic adjacent segment degeneration requiring surgery in patients after posterior lumbar fusion. J Orthop Surg Res. 2014 Dec;9(1):97.

81. Senteler M, Weisse B, Rothenfluh DA, Farshad MT, Snedeker JG. Fusion angle affects intervertebral adjacent spinal segment joint forces-Model-based analysis

of patient specific alignment: PREDICTED INTERVERTEBRAL JOINT FORCES AFTER FUSION. J Orthop Res. 2017 Jan;35(1):131–139.

82. Rothenfluh DA, Mueller DA, Rothenfluh E, Min K. Pelvic incidence-lumbar lordosis mismatch predisposes to adjacent segment disease after lumbar spinal fusion. Eur Spine J. 2015 Jun;24(6):1251–1258.

83. Schwab F, Ungar B, Blondel B, Buchowski J, Coe J, Deinlein D, DeWald C, Mehdian H, Shaffrey C, Tribus C, Lafage V. Scoliosis Research Society—Schwab Adult Spinal Deformity Classification: A Validation Study. Spine. 2012 May;37(12):1077–1082.

84. Eltes PE, Kiss L, Bereczki F, Szoverfi Z, Techens C, Jakab G, Hajnal B, Varga PP, Lazary A. A novel three-dimensional volumetric method to measure indirect decompression after percutaneous cement discoplasty. Journal of Orthopaedic Translation. 2021 May;28:131–139.

85. Rosenberg WS, Mummaneni PV. Transforaminal Lumbar Interbody Fusion: Technique, Complications, and Early Results. 2001;48(3):7.

86. Cole CD, McCall TD, Schmidt MH, Dailey AT. Comparison of low back fusion techniques: transforaminal lumbar interbody fusion (TLIF) or posterior lumbar interbody fusion (PLIF) approaches. Curr Rev Musculoskelet Med. 2009 Jun;2(2):118–126.

87. Ghasemi AA. Adjacent segment degeneration after posterior lumbar fusion: An analysis of possible risk factors. Clinical Neurology and Neurosurgery. 2016 Apr;143:15–18.

88. Maragkos GA, Atesok K, Papavassiliou E. Prognostic Factors for Adjacent Segment Disease After L4-L5 Lumbar Fusion. Neurosurgery. 2019 Jun 27;nyz241.

89. Fardon DF, Williams AL, Dohring EJ, Murtagh FR, Gabriel Rothman SL, Sze GK. Lumbar disc nomenclature: version 2.0. The Spine Journal. 2014 Nov;14(11):2525–2545.

90. Aryanto KYE, Oudkerk M, van Ooijen PMA. Free DICOM de-identification tools in clinical research: functioning and safety of patient privacy. Eur Radiol. 2015 Dec;25(12):3685–3695.

91. Bozic KJ, Keyak JH, Skinner HB, Bueff UH, Bradford DS. Three-Dimensional Finite Element Modeling of a Cervical Vertebra: An Investigation of Burst Fracture Mechanism. Journal of Spinal Disorders. 1994 Apr;7(2):102–110.

92. Zou KH, Warfield SK, Bharatha A, Tempany CMC, Kaus MR, Haker SJ, Wells WM, Jolesz FA, Kikinis R. Statistical validation of image segmentation quality based on a spatial overlap index1. Academic Radiology. 2004 Feb;11(2):178–189.

93. Bharatha A, Hirose M, Hata N, Warfield SK, Ferrant M, Zou KH, Suarez-Santana E, Ruiz-Alzola J, D'Amico A, Cormack RA, Kikinis R, Jolesz FA, Tempany CMC. Evaluation of three-dimensional finite element-based deformable registration of pre- and intraoperative prostate imaging. Med Phys. 2001 Dec;28(12):2551–2560.

94. Cignoni P, Callieri M, Corsini M, Dellepiane M, Ganovelli F, Ranzuglia G. MeshLab: an Open-Source Mesh Processing Tool. :8.

95. Fairbank JC, Couper J, Davies JB, O'Brien JP. The Oswestry low back pain disability questionnaire. Physiotherapy. 1980;66(8):271–273.

96. Valasek T, Varga PP, Szövérfi Z, Kümin M, Fairbank J, Lazary A. Reliability and validity study on the Hungarian versions of the Oswestry Disability Index and the Quebec Back Pain Disability Scale. Eur Spine J. 2013 May;22(5):1010–1018.

97. Gould D, Kelly D, Goldstone L, Gammon J. Examining the validity of pressure ulcer risk assessment scales: developing and using illustrated patient simulations to collect the data INFORMATION POINT: Visual Analogue Scale. J Clin Nurs. 2001 Sep 15;10(5):697–706.

98. Cicchetti DV, Shoinralter D, Tyrer PJ. The Effect of Number of Rating Scale Categories on Levels of Interrater Reliability : A Monte Carlo Investigation. Applied Psychological Measurement. 1985 Mar;9(1):31–36.

99. Dindo D, Demartines N, Clavien PA. Classification of Surgical Complications: A New Proposal With Evaluation in a Cohort of 6336 Patients and Results of a Survey. Annals of Surgery. 2004 Aug;240(2):205–213.

100. Ostelo RWJG, Deyo RA, Stratford P, Waddell G, Croft P, Von Korff M, Bouter LM, de Vet HC. Interpreting Change Scores for Pain and Functional Status in Low Back Pain: Towards International Consensus Regarding Minimal Important Change. Spine. 2008 Jan;33(1):90–94.

101. Beyer F, Geier F, Bredow J, Oppermann J, Eysel P, Sobottke R. Influence of spinopelvic parameters on non-operative treatment of lumbar spinal stenosis. THC. 2015 Oct 27;23(6):871–879.

102. Chapman TM, Baldus CR, Lurie JD, Glassman SD, Schwab FJ, Shaffrey CI, Lafage V, Boachie-Adjei O, Kim HJ, Smith JS, Crawford CH, Lenke LG, Buchowski JM, Edwards C, Koski T, Parent S, Lewis S, Kang DG, McClendon J, Metz L, Zebala LP, Kelly MP, Spratt KF, Bridwell KH. Baseline Patient-Reported Outcomes Correlate Weakly With Radiographic Parameters: A Multicenter, Prospective NIH Adult Symptomatic Lumbar Scoliosis Study of 286 Patients. Spine. 2016 Nov 15;41(22):1701–1708.

103. Eskilsson K, Sharma D, Johansson C, Hedlund R. The impact of spinopelvic morphology on the short-term outcome of pedicle subtraction osteotomy in 104 patients. Journal of Neurosurgery: Spine. 2017 Jul;27(1):74–80.

104. Simon J, Longis PM, Passuti N. Correlation between radiographic parameters and functional scores in degenerative lumbar and thoracolumbar scoliosis. Orthopaedics & Traumatology: Surgery & Research. 2017 Apr;103(2):285–290.

105. Castellvi AE, Nienke TW, Marulanda GA, Murtagh RD, Santoni BG. Indirect Decompression of Lumbar Stenosis With Transpsoas Interbody Cages and

Percutaneous Posterior Instrumentation. Clinical Orthopaedics & Related Research. 2014 Jun;472(6):1784–1791.

106. Malham GM, Parker RM, Goss B, Blecher CM. Clinical results and limitations of indirect decompression in spinal stenosis with laterally implanted interbody cages: results from a prospective cohort study. Eur Spine J. 2015 Apr;24(S3):339–345.

107. Pereira EAC, Farwana M, Lam KS. Extreme lateral interbody fusion relieves symptoms of spinal stenosis and low-grade spondylolisthesis by indirect decompression in complex patients. Journal of Clinical Neuroscience. 2017 Jan;35:56–61.

108. Endo K, Suzuki H, Tanaka H, Kang Y, Yamamoto K. Sagittal spinal alignment in patients with lumbar disc herniation. Eur Spine J. 2010 Mar;19(3):435–438.

109. Kiss L, Varga PP, Szoverfi Z, Jakab G, Eltes PE, Lazary A. Indirect foraminal decompression and improvement in the lumbar alignment after percutaneous cement discoplasty. Eur Spine J. 2019 Jun;28(6):1441–1447.

110. Navarro-Ramirez R, Berlin C, Lang G, Hussain I, Janssen I, Sloan S, Askin G, Avila MJ, Zubkov M, Härtl R. A New Volumetric Radiologic Method to Assess Indirect Decompression After Extreme Lateral Interbody Fusion Using High-Resolution Intraoperative Computed Tomography. World Neurosurgery. 2018 Jan;109:59–67.

111. Gates TA, Vasudevan RR, Miller KJ, Stamatopoulou V, Mindea SA. A novel computer algorithm allows for volumetric and cross-sectional area analysis of indirect decompression following transpsoas lumbar arthrodesis despite variations in MRI technique. Journal of Clinical Neuroscience. 2014 Mar;21(3):499–502.

112. Tsuji T, Watanabe K, Hosogane N, Fujita N, Ishii K, Chiba K, Toyama Y, Nakamura M, Matsumoto M. Risk factors of radiological adjacent disc

degeneration with lumbar interbody fusion for degenerative spondylolisthesis. Journal of Orthopaedic Science. 2016 Mar;21(2):133–137.

113. Ma Z, Huang S, Sun J, Li F, Sun J, Pi G. Risk factors for upper adjacent segment degeneration after multi-level posterior lumbar spinal fusion surgery. J Orthop Surg Res. 2019 Dec;14(1):89.

114. Kumar MN, Jacquot F, Hall H. Long-term follow-up of functional outcomes and radiographic changes at adjacent levels following lumbar spine fusion for degenerative disc disease. Eur Spine J. 2001 Aug;10(4):309–313.

115. Yilgor C, Sogunmez N, Boissiere L, Yavuz Y, Obeid I, Kleinstück F, Pérez-Grueso FJS, Acaroglu E, Haddad S, Mannion AF, Pellise F, Alanay A. Global Alignment and Proportion (GAP) Score: Development and Validation of a New Method of Analyzing Spinopelvic Alignment to Predict Mechanical Complications After Adult Spinal Deformity Surgery. The Journal of Bone and Joint Surgery. 2017 Oct 4;99(19):1661–1672.

116. Schwab FJ, Blondel B, Bess S, Hostin R, Shaffrey CI, Smith JS, Boachie-Adjei O, Burton DC, Akbarnia BA, Mundis GM, Ames CP, Kebaish K, Hart RA, Farcy JP, Lafage V. Radiographical Spinopelvic Parameters and Disability in the Setting of Adult Spinal Deformity: A Prospective Multicenter Analysis. Spine. 2013 Jun;38(13):E803–812.

10.Bibliography of the candidate's publications

10.1 Publications related to the thesis

Kiss L, Varga PP, Szoverfi Z, Jakab G, Eltes PE, Lazary A. (2019) Indirect foraminal decompression and improvement in the lumbar alignment after percutaneous cement discoplasty. Eur Spine J. 2019 Jun;28(6):1441-1447.

Eltes PE, **Kiss L**, Bereczki F, Szoverfi Z, Techens C, Jakab G, Hajnal B, Varga PP, Lazary A. (2021) A novel three-dimensional volumetric method to measure indirect decompression after percutaneous cement discoplasty. J Orthop Translat. 2021 Apr 1;28:131-139.

Kiss L, Szoverfi Z, Bereczki F, Eltes PE, Szollosi B, Szita J, Hoffer Z, Lazary A (2022) Impact of patient-specific factors and spinopelvic alignment on the development of adjacent segment degeneration after short-segment lumbar fusion (under review)

10.2 Publications not related to the thesis

Kiss L, Varga PP, Szoverfi Z, Jakab G, Eltes PE, Lazary A. (2020) Answer to the Letter to the Editor of T. Xie et al. concerning "Indirect foraminal decompression and improvement in the lumbar alignment after percutaneous cement discoplasty" by Laszlo Kiss et al. (Eur Spine J; 28(6):1441-1447). Eur Spine J. 2020 Jan;29(1):200.

Kiss L, Varga PP, Szoverfi Z, Jakab G, Eltes PE, Lazary A. (2019) Answer to the Letter to the Editor of Wang H, et al. concerning "Indirect foraminal decompression and improvement in the lumbar alignment after percutaneous cement discoplasty" by Laszlo Kiss et al. (Eur Spine J; 28(6):1441-1447). Eur Spine J. 2019 Dec;28(12):3093.

Eltes PE, Bartos M, Hajnal B, Pokorni AJ, **Kiss L**, Lacroix D, Varga PP, Lazary A. (2021) Development of a Computer-Aided Design and Finite Element Analysis Combined Method for Affordable Spine Surgical Navigation With 3D-Printed Customized Template. Front Surg. 2021 Jan 25;7:583386.

Eltes PE, **Kiss L**, Bartos M, Gyorgy ZM, Csakany T, Bereczki F, Lesko V, Puhl M, Varga PP, Lazary A. (2020) Geometrical accuracy evaluation of an affordable 3D printing technology for spine physical models. J Clin Neurosci. 2020 Feb;72:438-446.

Eltes PE , **Kiss L**, Bartos M, Eosze Z, Szoverfi Z, Varga PP, Lazary A. (2019) Attitude of spine surgeons towards the application of 3D technologies - a survey of AOSpine members. Ideggyogy Sz. 2019 Jul 30;72(7-8):227-235. English.

Lazary A, Klemencsics I, Szoverfi Z, **Kiss L**, Biczo A, Szita J, Varga PP. (2021) Global Treatment Outcome after Surgical Site Infection in Elective Degenerative Lumbar Spinal Operations. Surg Infect (Larchmt). 2021 Mar;22(2):193-199.

Szita J, **Kiss L**, Biczo A, Feher K, Varga PP, Lazary A. (2020) Outcome of group physical therapy treatment for non-specific low back pain patients can be predicted with the cross-culturally adapted and validated Hungarian version STarT back screening tool. Disabil Rehabil. 2020 Jul 31:1-9.

DOI:10.14753/SE.2022.2689

11. Acknowledgements.

I would like to express my sincere gratitude to my supervisor Dr. Áron Lazáry, his enthusiasm, knowledge, suggestions and exacting attention to details made me present this research work to produce in the present form. Sincere gratitude is extended to Dr. Péter Pál Varga, his generous participation in guiding, constructive feedback, kind support, and advice during my PhD.

This dissertation would not have been possible without the support of many people.
Very special thanks to team mates in R&D department, Julia Szita, Edit Pap, Dr. Ádám Biczó, Dr. István Klemencsics and Dr. Zsolt Szövérfi. Further, yet importantly, sense of respect goes to members of In silico Biomechanics Laboratory, especially Dr. Peter Endre Éltes for his guidance, Dr. Ferencz Bereczki, Maté Turbucz, Ágoston Pokori and Dr. Benjamin Hajnal for their help and support during the production of this thesis.
I also would like to thanks to all my respected colleges in Spine Surgery Department, National Center for Spinal Disorders, Dr. Balázs Szöllősi, Dr. András Bánk, Dr. Miklós Agócs, Dr. Zoltán Magor György, for their support, inspiration and cooperation in my study.

Last, but not least, my warm and heartfelt thanks go to my family especially Enikő for their tremendous support and hope they had given to me. Without that hope, this thesis would not have been possible. Thank you all for the strength you gave me.